In situ transmission electron microscopy investigation of the decomposition of the epitaxial GeSn layers

Šantić, Natalija

SVEUČILIŠTE JOSIPA JURJA STROSSMAYERA U OSIJEKU

ODJEL ZA KEMIJU

Diplomski studij kemije

NATALIJA ŠANTIĆ

In situ istraživanje termičkog raspada epitaksijalnih slojeva $Ge_{1-x}Sn_x$ legure transmisijskom elektronskom mikroskopijom

DIPLOMSKI RAD

OSIJEK, 2020

JOSIP JURAJ STROSSMAYER UNIVERSITY OF OSIJEK
DEPARTMENT OF CHEMISTRY
Graduate study of Chemistry

NATALIJA ŠANTIĆ

In situ transmission electron microscopy investigation of the decomposition of the epitaxial layer of $Ge_{1-x}Sn_x$ alloy

Supervisor:
Assist. Prof. Tomislav Balić

Co-supervisor:
DI Dr. Heiko Groiss

OSIJEK, 2020

TEMELJNA DOKUMENTACIJSKA KARTICA **Diplomski rad**

Sveučilište Josipa Jurja Strossmayera u Osijeku

Odjel za kemiju

Diplomski studij kemije, istraživački smjer

Znanstveno područje: Prirodne znanosti

Znanstveno polje: **Kemija**

In situ istraživanje termičkog raspada epitaksijalnih slojeva $Ge_{1-x}Sn_x$ legure transmisijskom elektronskom mikroskopijom

Natalija Šantić

Rad je izrađen na: Johannes Kepler University Linz, Centre of Surface and Nanoanalytics i Christian Doppler Laboratory for Nanoscale phase Transformations.

Mentor: Doc. dr. sc. Tomislav Balić

Komentor: DI Dr. Heiko Groiss

Sažetak: Legura $Ge_{1-x}Sn_x$ s x> 0,01 termodinamički je metastabilna i Sn na temperaturama iznad ≈230°C teži odvajanju, difundiranju i taloženju kao β-Sn u strukturama nalik kapljicama. In situ eksperimenti žarenja u transmisijskom elektronskom mikroskopu omogućuju promatranje i proučavanje termičkog raspada epitaksijalnih slojeva $Ge_{1-x}Sn_x$. Jedan od glavnih zahtjeva za ispitivanja putem TEM-a je uzorak proziran za elektrone. Prema tome priprema uzorka je ključni korak prema TEM pokusima. Postupak pripreme uzorka razvijen je kombinacijom različitih tehnika pripreme. Prvo, MBE sintetizirani $Ge_{1-x}Sn_x$ i referentni materijal Si (s Ge kvantnim točkama) pripremljeni su tehnikom klinastog poliranja. Nadalje, fokusirani ionski snop (FIB) korištena je za pripremu grijaćeg čipa za in situ eksperiment žarenja. Različite metode mikroskopije korištene su za optimizaciju i validaciju razvijenog postupka pripreme uzorka za in situ TEM eksperiment žarenja

Diplomski rad obuhvaća: 78 stranica, 39 slika, 3 tablice i 77 literaturnih navoda.

Jezik izvornika: Engleski jezik

Ključne riječi: fokusirani ionski snop / *in situ* eksperiment / klinasto poliranje / MEMS čip / priprema uzoraka / transmisijska elektronska mikroskopija

Rad prihvaćen:

Stručno povjerenstvo

1. doc. dr. sc. Tomislav Balić

2. izv. prof. dr. sc. Berislav Marković

3. doc. dr. sc. Aleksandar Szeczenyi

Rad je pohranjen: *Knjižnica Odjela za kemiju, Ulica cara Hadrijana 8/A, Osijek*

BASIC DOCUMENTATION CARD **Diploma Thesis**

Josip Juraj Strossmayer University of Osijek

Department of Chemistry

Graduate Study Chemistry; Research Study

Scientific Area: Natural Sciences

Scientific field: **Chemistry**

In situ transmission electron microscopy investigation of

the decomposition of epitaxial $Ge_{1-x}Sn_x$ layers

Natalija Šantić

Thesis completed at: Johannes Kepler University Linz, Centre of Surface and Nanoanalytics, and Christian Doppler Laboratory for Nanoscale phase Transformations.

Supervisor: Assist. Prof. Tomislav Balić

Co – Supervisor: DI Dr. Heiko Groiss

Abstract: The $Ge_{1-x}Sn_x$ alloy with $x>0.01$ is thermodynamically metastable and Sn tends to diffuse, segregate or precipitate as β-Sn in a droplet-like structure at temperature above ≈230°C. In situ heating experiments via transmission electron microscopy (TEM) allows us to observe and study the decomposition process of $Ge_{1-x}Sn_x$. The main requirement for TEM investigation is an electron transparent specimen. Hence, specimen preparation is a key step towards TEM experiments. The sample preparation procedure has been developed using a combination of preparation techniques. The MBE synthesized $Ge_{1-x}Sn_x$ and reference material Si (with Ge quantum dots) have been prepared with wedge polishing technique. Further, focused ion beam (FIB) has been used to prepare a heating chip for the in situ TEM heating experiment. Various microscopy methods have been used to optimize and validate the developed sample preparation procedure.

Thesis includes: 78 pages, 39 figures, 3 tables, and 77 references.

Original: English language

Key words: focused ion beam / *in situ* experiment / MEMS chip / sample preparation

/ transmission electron microscopy / wedge polishing

Thesis accepted:

Reviewers:

1. Tomislav Balić, Ph. D., Assist. Prof.

2. Berislav Marković, Ph. D., Assoc. Prof

3. Aleksandar Szeczenyi, Ph. D., Assist. Prof.

Thesis deposited in: *Library of the Department of Chemistry, Cara Hadrijana 8/A, Osijek*

I. Acknowledgment

Throughout the realization process of this thesis, I have received a great deal of support and assistance.

First and foremost, I would like to thank my supervisor Dr. DI Heiko Groiss for the given opportunity to work on my master's thesis project at Christian Doppler Laboratory for Nanoscale phase Transformation. I am truly grateful for guidance and patience through this six-month process.

I wish to express my sincere appreciation to Dr. Alexey Minenkov for the immense contribution during both the research and writing process of my thesis. His insightful feedback and stimulating discussions helped me to successfully conduct and complete my thesis.

I would like to thank all my colleagues at the CDL and ZONA for their support and passed knowledge, but also for their warm hospitality. Especially I would like to recognize my gratitude to DI Tia Truglas for invested time and effort during my Internship at ZONA and for giving me competent advice.

Although they might not truly understand what I am studying my very profound gratitude goes to my family. To my mother Vesna for believing in me and giving me tremendous amount of support. To my sisters Tajana and Iva for making me laugh through hard times. You are my biggest inspiration and motivation.
Family always and forever.

Thank you everyone!

What now?

Natalija

II. Abstract

The progressive development of high-performance transmission electron microscopy (TEM) needs constant development of the sample preparation approaches as it is one of the vital steps towards the TEM investigation.
In situ TEM experiments provide dynamic observation of the physical behaviour of materials in response to external stimuli such as temperature. The main goal of this thesis is to develop a suitable approach for the preparation of molecular beam epitaxy synthesized $Ge_{1-x}Sn_x$ sample and Si sample as reference for an in situ heating experiment. $Ge_{1-x}Sn_x$ sample has remarkable interest for *in situ* investigation since elevated temperature causes decomposition of the epitaxial layer. The decomposition process limits the material as a semiconductor material thus investigation of the decomposition process is of scientific and technological interest.

The preparation of the sample for *in situ* experiments offers many viable ways. We developed an elaborate preparation and analysis procedure by combining a mechanical wedge polishing procedure with a focused ion beam technique to prepare a thin lamella. The preparation workflow described in the thesis involves wedge preparation, FIB lamella preparation, and its subsequent transfer and welding to the MEMS-based nanochip. To validate and testify the developed approach scanning electron microscopy is used. Additionally, prepared MEMS chips are examined at room temperature via TEM. The result of the heating experiment of reference Si sample is presented and supported by the TEM sequence of images at the various annealing temperatures.

Based on the result of this study a novel preparation and examination procedure is given for an improved protocol for *in situ* heating specimen investigation.

III. List of abbreviations

Ac	Acetone
AFM	Atomic Force Microscopy
CMOS	Complementary Metal Oxide Semiconductor
DLF	Diamond Lapping Film
EtOH	Ethanol
FIB	Focused Ion Beam
GIS	Gas Injection System
IPA	Isopropyl alcohol
MBE	Molecular Beam Epitaxy
MEMS	Microelectromechanical system
QDs	Quantum Dots
SEM	Scanning Electron Microscopy
TEM	Transmission Electron Microscopy
VLM	Visible Light Microscope

IV. List of Figures

V. List of Tables

Table of content

1. Introduction and Motivation

The development and synthesis of novel materials must be guided by atomic-scale compositional and structural analysis. Transmission electron microscopy (*TEM*) is an excellent tool for the investigation of various materials and provides morphologic, compositional, and crystallographic information on samples. This Master's thesis presents the development and optimization of the novel approach in the sample preparation of a thin layer of $Ge_{1-x}Sn_x$ alloy including its subsequent installation on a cutting-edge MEMS-based chip for *in situ* TEM heating experiments.

The $Ge_{1-x}Sn_x$ nanoscale alloy is metastable and nonequilibrium entities, thus they require low-temperature synthesis and application processes to avoid decomposition.[1] The fundamental and applicational interest of $Ge_{1-x}Sn_x$ relies on recent experimental proof of lasing of $Ge_{1-x}Sn_x$ along with possible bandgap tunning and compatibility with Si-based technology. [2]–[4] Pure Germanium has an indirect bandgap that can be tuned to a direct gap by incorporating tin (Sn) into the germanium lattice to form a substitutional $Ge_{1-x}Sn_x$ alloy. Hence, the system has a prominent potential for application in photonics since recent experimental proof of lasing of $Ge_{1-x}Sn_x$. During the sample preparation of $Ge_{1-x}Sn_x$ alloy for TEM investigation, two properties of $Ge_{1-x}Sn_x$ must be considered the amount of strain and decomposition of $Ge_{1-x}Sn_x$ layers. The strain caused by the large lattice mismatch of 14.6% between Sn and Ge can lead to the cracking of the sample during sample preparation. Besides, the strain reduces the incorporation of Sn while growing $Ge_{1-x}Sn_x$ layer and leads to segregation and phase separation at ≈140-230 °C, which is even lower than the bulk eutectic temperature of the Ge/Sn system. Hence, one must be careful during sample preparation and does not reach the decomposition temperature The efficient phase separation results in a formation of Sn droplet-like structures on the surface [3],[5],[6], altering the desired material properties, thus, should be avoided.

Electron microscopy is a well-developed tool offering high-resolution imaging to obtain comprehensive information on microstructures at the nanoscale. Despite all the possibilities that TEM offers, sampling is a disadvantage, since only a small part

of the specimen can be observed at once.[7] In this sense, TEM should not be considered as a fundamental investigation technique rather a powerful complementary method.

Therefore, before analyzing the specimen with TEM, the quality of the prepared specimen should be examined by poorer resolution methods but with better sampling, e.g. by a naked-eye, Visible Light Microscope (*VLM*), Scanning Electron Microscopy (*SEM*), and Atomic Force Microscopy (*AFM*).

TEM is a technique based on an interaction of the accelerated beam of electrons transmitted through an ultra-thin specimen.[8] In this regard, the specimen preparation is an essential step in TEM investigations. The samples for the TEM study must be thin enough to be transparent for electrons, generally having a thickness of less than 100 nm, and at the same time, they should be prepared in an unharmful way, retaining the properties of the original material. [9]

Traditional specimen preparation techniques include surface replica, powder specimen preparation, film preparation for plan-view, the foil preparation from a bulk sample, and cleaving.[9] Classical sample preparation methods used are sawing, ultrasonic cutting, dimpling, mechanical polishing, electrolytic polishing, and chemical polishing.[10]

Practicing classical methods, it is possible to achieve a thin specimen with a flat and polished surface. These techniques are simple to conduct and they are quite inexpensive. The classical methods have significant drawbacks mainly because they are often time-consuming (several hours for one specimen) and require a well-equipped preparation laboratory, and heavy use of consumables. The artifacts that can be introduced by using the above-mentioned techniques are compression, stretching, and tearing all or part of a sample's volume. These can generate prominent changes in matter conformation and distribution.[10]

The advanced sample preparation techniques include cross-sectional specimen preparation, inorganic non-metallic material preparation, and special specimen preparation via Focused Ion Beam (FIB).[11],[12]

The conventional sample preparation includes classical methods usually followed by FIB milling. There are two main drawbacks:

1) Mechanical load from cutting and polishing causes changes in microstructures such as dislocations, strains, rupture, etc.

2) Additional Ion milling is usually required to achieve electron transparent regions in the sample, but has few flaws:
    - → The major problem is the implantation of argon ions in the sample leading to structural changes: formation of amorphous layer and phase transformations.
    - → Different sputtering rates of materials (the effectiveness of etching depends on the chemical nature of the material).[9]

To solve complex preparation challenges and obtain thin slices that can be analysed with TEM, a combination of several techniques is suggested. [10],[11]

In situ TEM is a suitable tool to understand the properties and the decomposition process of $Ge_{1-x}Sn_x$ alloy. *In situ* TEM means that the atomic or nanoscale observation can be performed application of different physical/chemical stimulus such as heating, which will be carried out with $Ge_{1-x}Sn_x$ samples. The heating experiments are performed by using specially designed TEM holders, the most advanced of which are equipped with MEMS-based heating chips. Thin specimen's preparation for conventional TEM is a difficult routine, which complicates even further for an *in situ* TEM investigation. The installation of a thin specimen on the MEMS chip is generally difficult. The $Ge_{1-x}Sn_x$ samples complicate the preparation procedure even more due to their metastability and the decomposition process that can occur.

Thrivingly, during the experimental work of this thesis, the challenges regarding the $Ge_{1-x}Sn_x$ preparation for *in situ* heating TEM experiment were successfully vanquished.

Thus, this master's thesis presents the elaborated and improved procedure for the preparation of MEMS-based chip with the following samples been installed: Si-wafers (both pure and with Ge-quantum dots) as reference material and metastable $Ge_{1-x}Sn_x$ alloy grown by molecular beam epitaxy (MBE) as a final goal.

A protocol for the mechanical wedge polishing technique is presented and the quality of produced samples is supported by VLM and SEM images. Additionally, the experimental steps to prepare the MEMS-heating chip with a specimen is described. The cutting, lift-out, and transfer of lamellae to MEMS chip with a FIB will be explained and presented with SEM/FIB images. The preparation process was optimized and validated by AFM, optical microscope, SEM experiments. The results of the first *in situ* heating TEM experiment are presented and discussed.

2. Theoretical Background

In this chapter, the theoretical background that is crucial for understanding the overall content of the thesis is presented. A general introduction will be given regarding the growth of $Ge_{1-x}Sn_x$ samples. The importance of Electron microscopy in Material Science with outlined properties of electrons and their interaction with matter is presented as well.

The conventional preparation techniques and the novel approach for the TEM sample preparation will be discussed. Challenges that may occur during the preparation process and that should be overcome will be described.

2.1. Si- $Ge_{1-x}Sn_x$ Systems

2.1.1. Physical Properties

The so-called elemental semiconductors, Si and Ge, are common and belong to the Group-IV of the periodic table. The most widely used and examined one is silicon. One of the restrictions of Si-based technology is that Si's indirect bandgap limits its use in optoelectronics.[13] Thus, integration of another direct bandgap material onto silicon is required for on-chip optoelectronics. In this regard, $Ge_{1-x}Sn_x$ alloys look exceedingly perspective. Recently, plentiful scientific researches have demonstrated lasing in $Ge_{1-x}Sn_x$ alloys.[2],[3],[14] Additionally, $Ge_{1-x}Sn_x$ alloys stand out due to the high electron and hole mobility property and are suitable for high-speed CMOS devices.[15]

Si, Ge, and α-Sn have a diamond cubic structure presented in Figure 1. a). The diamond lattice can be formed from two face-centered-cubic Bravais lattices, which are displaced along the body diagonal of the larger cube by one-quarter of that body diagonal (see Figure 1. b)).

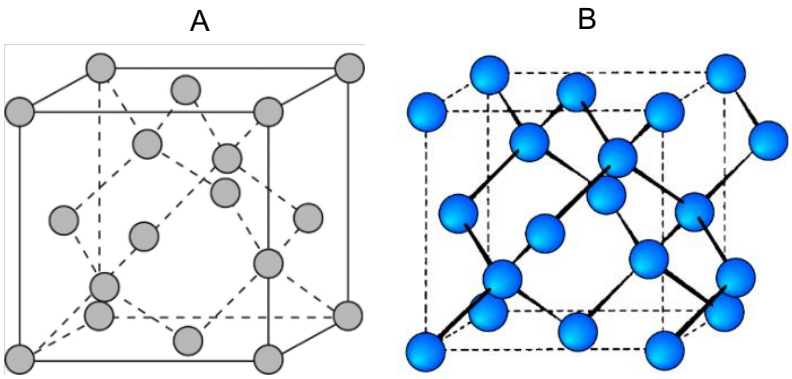

Figure 1. *a) The diamond cubic lattice; b) The unit cell structure of a diamond cubic lattice showing the two-interpenetrating face-centered cubic lattices.* [16]

The lattice mismatch between Si and Ge is 4.2% since the lattice constant of Si, (a_{Si}), is 0.543 nm and the lattice constant of Ge, (a_{Ge}) is 0.566 nm as *Table 1.* shows. Silicon and germanium are fully miscible and form a solid solution $Si_{1-x}Ge_x$ with x ranging from 0 to 1. [17]

Table 1. *Structural and electronic properties for the diamond cubic forms of the group IV (14) elements.[18]-[20]*

Element	**Lattice parameter, a [nm]**	**Melting point [K]**	**Indirect bandgap [eV] at 300 K**
Carbon (diamond)	0.35668	-	5.50
Silicon	0. 5431	1687	1.1242
Germanium	0.5658	1211	0.664
α-Tin	0.6489	505	-

Electrons in a semiconductor material are eighter in the ground energy state in the valence band or excited as charge carriers in the conduction band. The range of forbidden energies between defines the bandgap. The material's bandgap is determined by its molecular structure. The band structure defines if a semiconductor material is direct or indirect. If the highest state of the valence band (valence band maximum) and lowest state of the conduction band (conduction band minimum) are placed on top of each other, the material is a direct bandgap semiconductor.[18] Compared to Si pure Ge has a narrow indirect bulk bandgap of 0.66 eV at 300 K. Application of tensile strain or alloying with other elements, for example, Sn, can tune the band structure, thus change optical and electrical properties. This can be done with Ge and it can become a direct semiconductor.[19],[20]–[22]. Incorporation of Sn into Ge lattice to form $Ge_{1-x}Sn_x$ alloys results in a similar effect as observed in

Ge under tensile strain. This results in lowering the energy of the conduction band and overlapping with the valence band leading to a direct bandgap.[8],[9],[54] To achieve this a high concentration of Sn (above 9 at%) is necessary.[23] In contrast to Si-Ge, which are completely miscible, the solid solubility of Sn in Ge is extremely low (x_{sl} ≈1%).[3],[24] Moreover, α-Sn is thermodynamically stable only below 13.2 °C, at room temperature tin exists as its β allotrope, also knowns as white tin with a body-centered tetragonal crystal structure.[27],[28] Only α-Sn could be considered as semiconducting material, therefore the α→β phase transformation of Sn is detrimental in the majority of device applications. To fabricate $Ge_{1-x}Sn_x$ alloys the huge lattice mismatch between α-Sn and Ge of 14.7% and low solubility must be overcome.

2.1.2. Material synthesis

The phase diagram of the $Ge_{1-x}Sn_x$ system constructed by Olesinski R., et. al. [15], is shown in Figure 2. The diagram shows that the eutectic temperature of Ge–Sn binary alloys are as low as 231.1 °C close to the one of pure Sn (231.5°C).[6], [15], [27] Three stable $Ge_{1-x}Sn_x$ phases can be formed under equilibrium conditions: 1) the liquid phase that can be formed at a temperature beyond 938,3 °C, 2) the solid solution of α-Sn in Ge, and 3) the solid solution of Ge in β-Sn. According to the diagram, the maximum solid solubility of Sn in Ge is about 1.1 at% Sn at a temperature of 400 °C. While the solubility at room temperature is approximately 0.5 at% Sn.

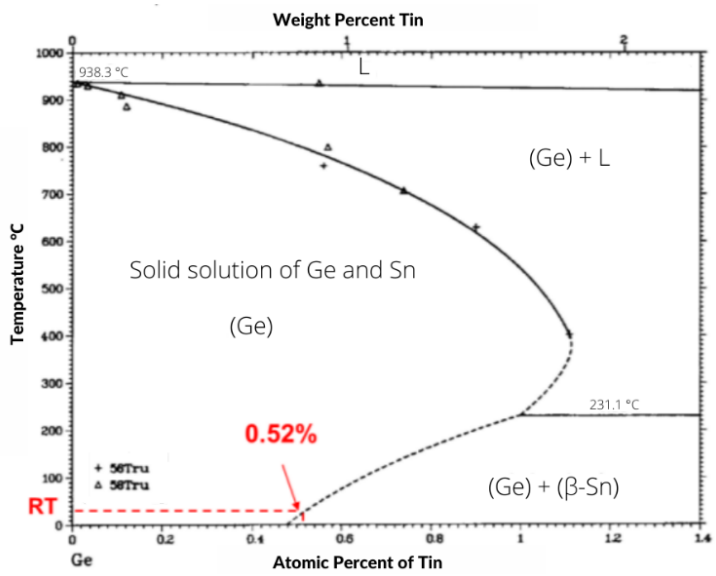

Figure 2. *Phase diagram of the* $Ge_{1-x}Sn_x$ *system under equilibrium conditions.*[15]

The lattice mismatch of α-Sn and Ge according to literature is 14.7%.[28],[30],[31] Thus, the Ge-$Ge_{1-x}Sn_x$ heterostructures experience a large amount of compressive strain. This provides a tool for band-structure engineering, as was previously pointed out. But, when the thickness of the $Ge_{1-x}Sn_x$ layer reaches a threshold value the epitaxial strain energy is relieved by the generation of dislocation.[31] This relaxation can partly or fully lead to equilibrium lattice spacing. The growth of single-crystal $Ge_{1-x}Sn_x$ alloy requires lattice-matched substrates.[32]For a technological relevance of $Ge_{1-x}Sn_x$ alloy, epitaxial growth on Ge or Ge-on-Si substrate is required.[17], [27], [32], [33]

As previously stated, at 13.2 °C α-Sn experience an allotropic phase transition from diamond lattice to the tetragonal lattice of metallic β-Sn. $Ge_{1-x}Sn_x$ with $x>0.01$ is thermodynamically metastable and Sn tends to diffuse, segregate or precipitate as β-Sn in a droplet-like structure.[3][34]–[36]

Atomic force microscopy is an excellent tool that has been used to gain more information about the annealing impact of the $Ge_{1-x}Sn_x$ sample. Figure 3. presents the surface topography of post-annealed $Ge_{1-x}Sn_x$ samples. One can distinguish two deep tranches with a “fish-bone” pattern (in the right image) caused by a movement of Sn droplets on the $Ge_{1-x}Sn_x$ surface. A part of the intact original surface can be seen, as well as formed Sn droplets (white entities).

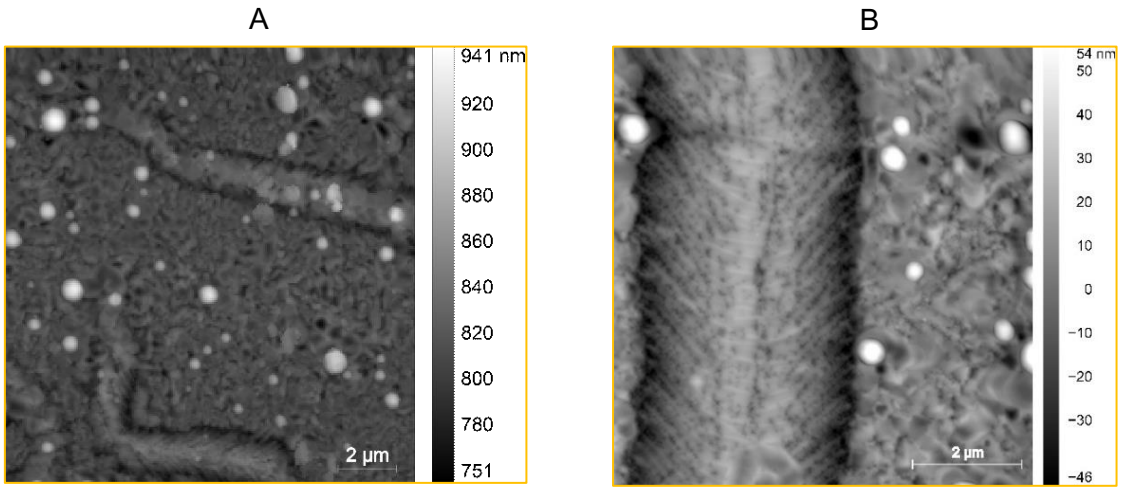

Figure 3. *Non-contact mode AFM imaging of a post-annealed sample of* $Ge_{1-x}Sn_x$*. Morphological features such as deep trenches and island-like structures are visible in both images (A and B).*

It is difficult to increase the Sn content in $Ge_{1-x}Sn_x$ because the Sn precipitation from the $Ge_{1-x}Sn_x$ matrix easily occurs at a low temperature during the crystal growth and post-growth processes [36]–[38] The segregation is dependent on the concentration of Sn in $Ge_{1-x}Sn_x$ alloy.[39] Therefore, to achieve a supersaturated solid solution of Sn in Ge and avoid Sn precipitation, material growth needs to be carried out at conditions far from equilibrium. The common fabrication methods of $Ge_{1-x}Sn_x$ alloys are chemical vapor deposition (CVD), molecular beam epitaxy (MBE), sputtering deposition, solid-phase epitaxy, and pulsed laser deposition.

The experiment and the study in the frame of this thesis will be conducted with the MBE synthesized $Ge_{1-x}Sn_x$ sample. MBE is an epitaxial method used for the preparation of advanced structures with composition and doping profiles controlled on an atomic (monolayer of atoms) scale. MBE process of the growth of materials takes place under ultrahigh vacuum conditions on a heated crystalline substrate.[29],[30]

The ultrahigh vacuum environment secures high purity, and the MBE process allows the preparation of a clean surface with specific reconstruction. One of the most notable aspects of MBE is the deposition rate (usually less than 3000 nm/h) that allows the films to grow epitaxially.[40] Epitaxy refers to a type of crystal growth or material deposition in which new crystalline layers are formed with one or more well-defined orientations with respect to the crystalline substrate.[42]

The description of the MBE fabricated sample will be provided in the Experimental Chapter of the thesis. The next section will focus on general sample preparation techniques for Electron microscopy investigation.

2.2. Methods and Instruments

In the following Chapter, the relevant techniques concerning the preparation and characterization of the samples for the master's thesis will be described. The main samples requirement for TEM investigation will be given.

2.2.1. Electron microscopy

Electron microscopy (EM) brought revolutionary approaches for imaging technology for scientists and engineers leading to the opening of a new field of research on the nanoscale of materials thus enabling characterization of unique and prominent properties. EM was developed as an answer to limiting image resolution of a visible light microscope (VLM). EM is the essential methodology to determine the morphology, crystal and defect structure, elemental composition, and electronic properties of materials.[43] The general principle underlying electron microscopy techniques is the interaction between an electron beam and the atoms of a target sample in a vacuum.

There are two types of electron microscopes - transmission electron microscopes (TEM) and scanning electron microscopes (SEM). SEM shows the specimen surface thus a bulk sample can be examined, and sample preparation is simplified. TEM is used to view thin specimens through which electrons can pass generating a projection image. The sub-surface crystal quality and defect characterization can be obtained from TEM.

2.2.1.1. Interaction of Electrons and Specimen

Electrons have a strong interaction with matter producing various signals that can be traced with an appropriate detector.[44]

Figure 4. depicts all the signal which are generated from the interaction of the electron beam and specimen. Scattering of electrons can be classified as *elastic* if results in no loss of energy and *inelastic* if the kinetic energy of electron changes.

Elastically scattered electrons can change direction but do not change their wavelength. Scattering angle can take all values from 0° to 180° from the initial direction.

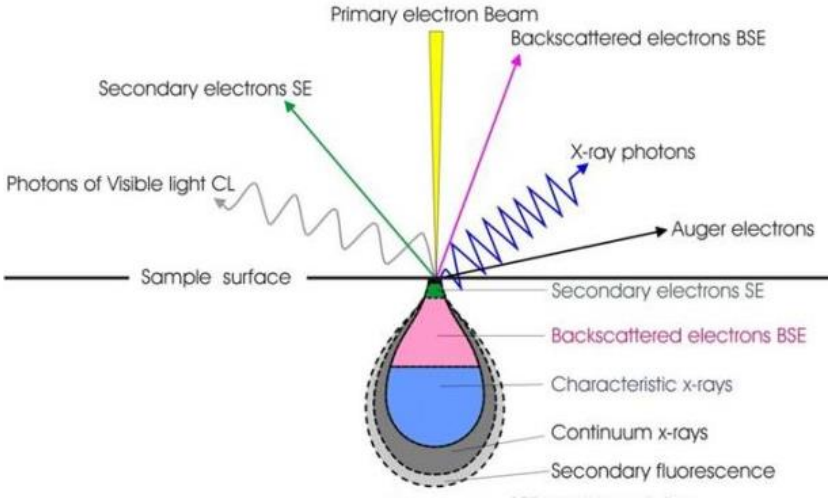

Figure 4. *Signal generated from the interaction of a high-energy beam and thin specimen.*

Some of the primary electrons are diffracted by a crystalline specimen due to the wave nature of the electrons. This effect is especially important for the transmitted electron beams of thin specimens used in TEM.

Moreover, elastic scattering happens if the electron is deflected from its path by Coulomb interaction with the positive potential inside the electron cloud. The Coulombic force is defined as $F = \frac{Q_e Q_n}{4\pi\varepsilon_0 r^2}$, where *Q* is the charges of electron and nucleus, *r* is the distance between charges, and ε_0 is the dielectric constant. The closer the electron comes to the nucleus, the smaller the r is, thus the larger are *F* and the scattering angle. If the distance *r* is small enough, complete backscattering can occur generating back-scattered electrons (BSE) that are elastically scattered through an angle of more than 90˚.

In the inelastic scattering, the energy from the incident electrons is transferred to the specimen and is reduced ($E_{el} < E_0$) by several mechanisms. Inelastically scattered electrons have a longer wavelength. This can result in different kinds of secondary signals like Auger electron (AE), secondary electron (SE), characteristic X–rays, phonons, plasmons, or cathodoluminescence.

SEs that are ejected from the conduction or valance band of the specimen by a small amount of energy are referred as to slow SE and carry energies below 50 eV. These are utilized in SEM forming images of morphology and surface topography. When a primary electron has enough energy, it can eject the inner shell electrons that are more strongly bounded and less readily ejected. This generates characteristic X-rays or Auger electrons which are another kind of SE (fast SEs).

2.2.2. Scanning Electron microscopy

Scanning electron microscopes (SEM) produce images of a sample by scanning it with a focused beam of electrons across the specimen surface using deflection/scanning coils.[45] The electron gun which is located on top of the microscope's column emits electrons. The electrons are then accelerated to energy levels up to 30 keV. Electromagnetic lenses and apertures are used for focusing and deflection of the electron beam to form a small, concentrated electron spot on the sample. This beam is controlled in a raster-scanned fashion in the X-Y direction onto the sample surface When the deflection angle is changed, the scanned area will change, resulting in higher magnifications for smaller deflection angles.[46]

Backscattered electrons that are reflected from the incident beam and Secondary electrons from inelastic interactions between the electron beam and the sample are the main signals used in SEM. BSEs are scattered from the sample with small energy loss and can travel deeper withing the sample, meanwhile, SE originates from surface regions. Hence, they carry different types of information.[47] The number of backscattered electrons emitted from a specimen is dependent upon the atomic number of the specimen.

BSE resolves topographical contrast and atomic number contrast with a resolution of <1 micron.[47],[48] Materials with higher atomic numbers produce brighter images.[45] SE imaging is the basic imaging mode and SEs are very useful for the inspection of the topography of the sample's surface. Different detectors and detector mode can be used to collect and operate SE/BSE electrons/signals. Everhart-Thornley (ET) detector is used for SE and it is usually fitted on one side of the vacuum chamber.[47] SE signal intensity can be enhanced by tilting the specimen toward the detector. BSE can be as well detected by ET detector. The other common BSE detectors are solid-state detectors which are usually placed above the sample in an arrangement that maximizes the collection of BSEs.

Large samples of few centimetres are acceptable for SEM analysis, up to 3-20 cm in diameter, depending on the stage installed within the SEM chamber.[47] The specimen must be electrically conducting, if not, it can be coated with common metallic capping layers such as aluminium, gold, platinum, chromium, tungsten, tantalum, and palladium.[49] The specimen must have all volatile materials removed from it to not degrade the vacuum of the SEM. SEM was a valuable technique for the optimization of the GeSn samples preparation technique. The ZEISS 1540XB-Crossbeam SEM with Focused ion beam (FIB) add-on available at the *Centre for Surface and Nanoanalytics* was used to obtain insights on the surface topography of wedge polished GeSn sample to better understand the preparation procedure. Further, FIB add-on was used for the cutting of thin GeSn specimen (lamella), its transfer to MEMS-heating chip, and for final thinning.

2.2.3. Transmission Electron microscopy

The working principle of TEM can be compared to an optical microscope where photons are replaced with electrons and glass lenses with electromagnetic ones, respectively.[50] TEM allows the crystallographic and chemical characterization of materials with an outstanding spatial resolution of 2 nm, or even better with C_s-corrected instruments (resolution of 23 pm).

A simplified sketch of a TEM setup is presented in Figure 5. The electron gun, which is located at the top of the TEM, emits electrons that are accelerated with a high voltage (typically 80-300 keV). A beam of electrons is transmitted through a thin specimen, interacting with the specimen as it passes through. The transmission of electrons is a function of the thickness and elemental composition. More electron-dense regions of the specimen allow fewer electrons to be transmitted and appear darker, conversely thinner area and those containing lighter elements permit more transmission and appear lighter. From this, the morphological features such as the size, shape, and arrangement of the particles can be distinguished.

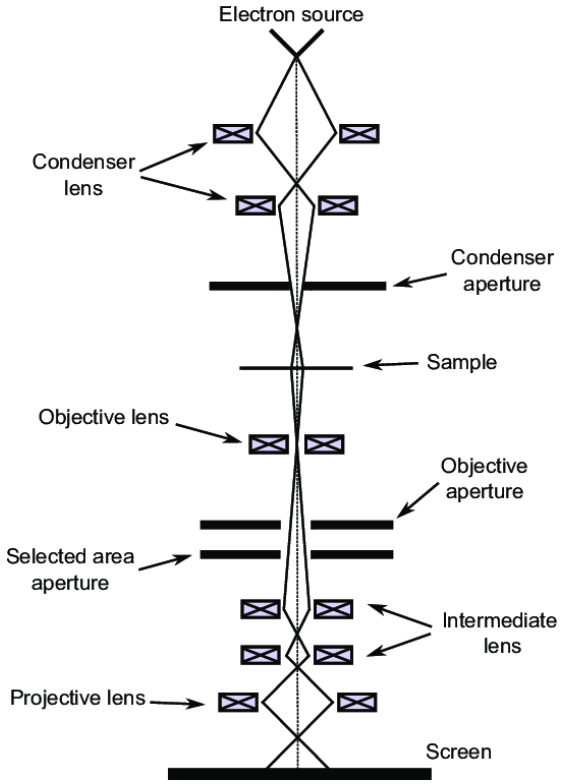

Figure 5. *A simplified schematic diagram of a Transmission electron microscope.*

All the basic operations in TEM are realized with the help of lenses. There are four systems of lenses generally used in the TEM for different purposes: condenser lens, objective lens, intermediate lenses, and projector lenses.[51]

An aperture is used in lenses to control the beam current and convergence angle of the beam hitting the specimen. Condenser lenses are used to create either a convergent or a parallel beam of electrons. The beam then hits the specimen, and it is transmitted depending upon the thickness and electron transparency of the specimen. The transmitted beam is focused by the objective lens into an image onto a fluorescent screen, on a layer of photographic film, or it can be viewed by a CCD (charge-coupled device camera). Additional objective apertures can be used to enhance the contrast by reducing/blocking out high -angle diffracted electrons. The image then passes down the column through the intermediate and projector lenses and it is enlarged.

TEM can be used for conventional and high-resolution images, electron energy-filtered imaging, electron diffraction, scanning (S)TEM, and quantitative element investigation with energy-dispersive X-ray spectroscopy.[7] Conventional TEM's primarily act as an imaging tool to characterize structures of materials and it is unable to replicate environmental conditions e.g. heating. The samples are completely static and are restricted to the ultra-high vacuum conditions present inside the TEM.[52] *In situ* transmission electron microscopy is a technique that allows the study of a sample's response to a stimulus in real-time. *In situ* observation of dynamic processes can provide real-time interactions between materials and apply external fields or environments, including thermal, electrical, mechanical, liquid/gas environmental, optical excitation, and magnetic fields.[53], [54] Recently, *in situ* investigation has become more accessible with the development of Micro-Electrical-Mechanical System (MEMS) devices to control the environmental condition of the sample.[55]

Jeol JEM-2200FS was used to carry out the *in situ* TEM heating experiment of the GeSn samples. This TEM is equipped with a Field Emission Gun (FEG) that can be operated between 80-200 kV acceleration voltage and with the in-column energy filter that allows a zero-loss image eliminating inelastic electrons resulting in clear images.[56]

2.2.4. General preparation techniques for Electron microscopy

As was stated previously in brief, the characterization of materials using TEM requires specimens that are thin enough so that they are electron transparent, therefore having a thickness between 30 to 100 nm, not exceeding 500 nm (depends on the nature of the material). Additionally, it is necessary to make the sample small enough to fit in the TEM specimen holder. The specimen should be either self-supported or mounted on a grid. The standard sample support grid (*see Figure 6. b*)) sizes are ~ 3 mm in diameter and commonly made of copper. [7]

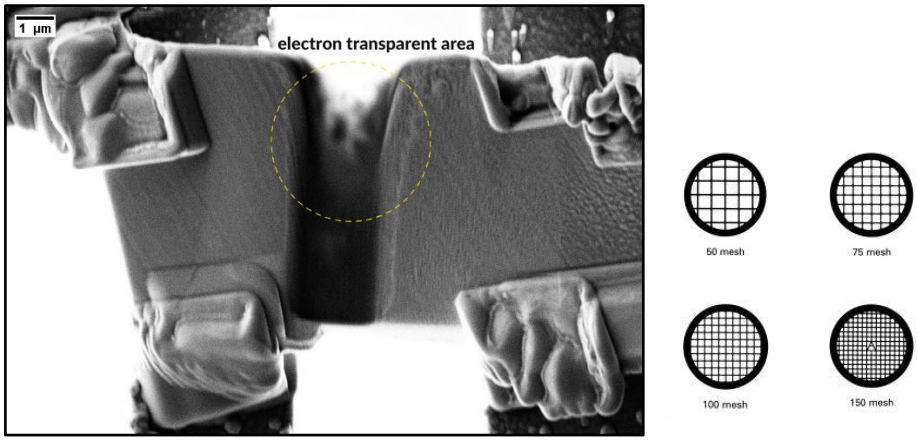

Figure 6. *a) SEM image of an electron transparent area of a FIB prepared lamella. The electron transparent area is brighter than the rest of the specimen. b) Different types of TEM grids.*

The preparation procedure should ensure a larger electron transparent area. The artifacts such as scratches, amorphization, decomposition should be avoided during the preparation. The sample should be stable enough to withstand handling. The sample preparation procedure should be reproducible, fast, and economic.[57] Besides the thickness, an ideal specimen should be flat, robust, homogenously thick, and clean.[10] The sample preparation is often time-consuming, requiring many instruments, and it needs regular improvement with the development of new material and approaches for their synthesis

When it comes to choosing the proper preparation technique the most suitable is the one that produces a convenient thin slice of material. The specimen must be applicable for different analyses.

The selection of the adequate method is based on the material's chemical, mechanical, or electrical properties. Further, information about the investigated sample defines the choice of the preparation technique. Extended criteria that must be considered are listed below:

1) Material type: metal, semiconductor, ceramic, minerals, biological material, polymer, mixed-composite material
2) Material geometry: bulk materials, thin layer, multilayer materials, and fine particles that include fibres, platelets, sphere, nanotubes, etc.
3) Physical structure: compact, porous, and in the liquid phase
4) Chemical phases: single-phase and multiphase
5) Hardness: hard, soft, fragile, ductile, heterogenous
6) Electrical properties: conductor or insulator.[57]

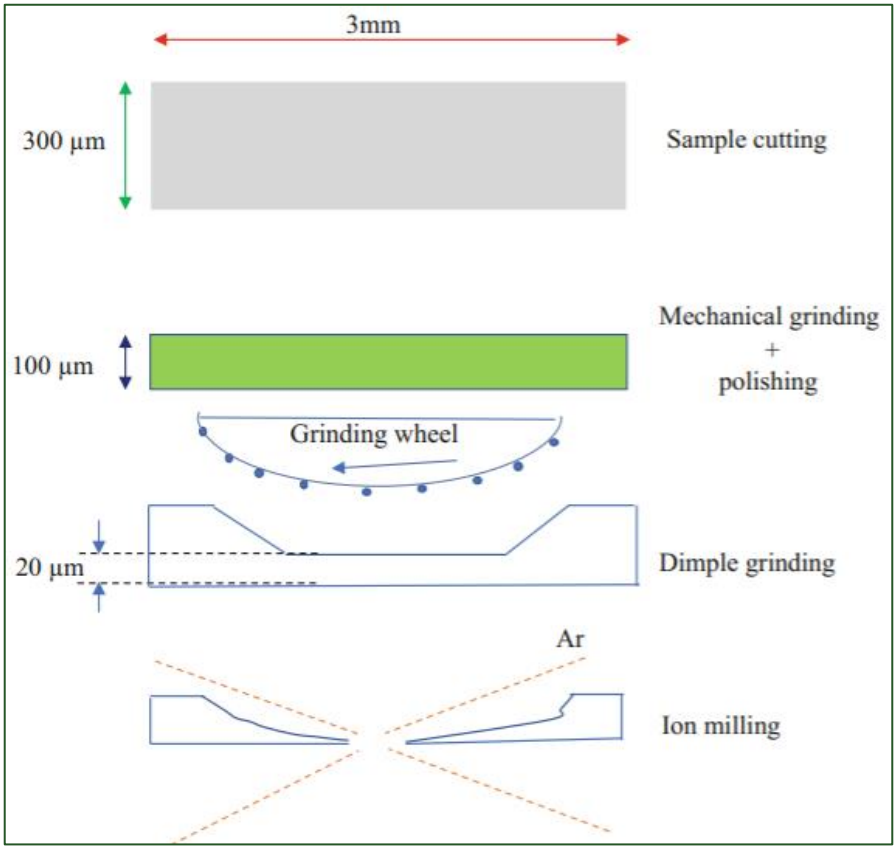

Figure 7. *Conventional TEM sample preparation workflow.*

Interaction mechanisms involved in the conventional sample preparation technique are abrasion or dissolution of the material. Preliminary preparation techniques used in materials science are sawing, ultrasonic cutting, dimpling, sandwich, mechanical polishing, electrolytic polishing, and chemical polishing. [9],[58]

Figure 7. represents a schematical workflow of the conventional sample preparation procedure. Bulk material must be resized to fit the TEM grid and holder, although for SEM investigation a bulk material can be mounted on an SEM holder without being cut to smaller dimensions. As it is presented in Figure 7. the preparation requires few steps involving different techniques and instruments which will be further described.

2.2.4.1. Sawing and Ultrasonic cutting

Sawing is performed with a wheel or a wire *(see Figure 8. A)* having different size and hardness of the abrasive grains (diamond, SiC, etc.). [10] Method strongly depends on material properties (hardness, ductility, brittleness). Cutting should ensure the minimal formation of artifacts associated with the cutting performance, the load applied to the sample, and generated heat during cutting, used chemicals (cutting liquid), and nature of the abrasive.

The WELL Diamond wire saw was used to cut out samples from MBE Si wafers and $Ge_{1-x}Sn_x$. This wire saw uses gravity and/or weight as the method for achieving and maintaining consistent feed rates. This ensures minimal force on the sample thus reducing potential damage to the sample during cutting. The stresses introduced by abrasion can cause cracks at different depths in the material even up to 200 μm.[58] Adequate handling of the wire saw and use of lubricant (alcohol or water) as a cooling agent can reduce the risk of the surface's damage, i.e. the load must be adjusted to the hardness of the material and the speed of the diamond wire can be adjusted. Usually, a larger sample or cross-sectional sample is cut into slides then a disk-shaped specimen is cut out with an ultrasonic cutting instrument.

Ultrasonic cutting is achieved using a cutting tool (*Figure 8. B*) attached to an ultrasonic generator, a motor-driven, rotating toothless bit (with an abrasive). A solution containing abrasive grains is placed on the surface of the sample.[10] The tool is moved to make full contact with the surface.

The ultrasonic cutter uses vibration and pressure applied to the surface to cut out samples into a disk-shaped one with suitable dimensions for TEM sample holders. Using this method to cut samples of a desirable shape has minor mechanical damage to the actual sample.[59] This instrument quickly cut a sample of unique shape from hard, brittle materials such as semiconductors, ceramics, etc. Using a manually tuned frequency driver to optimize cutting speed can thrivingly minimize mechanical and thermal damage.

A B

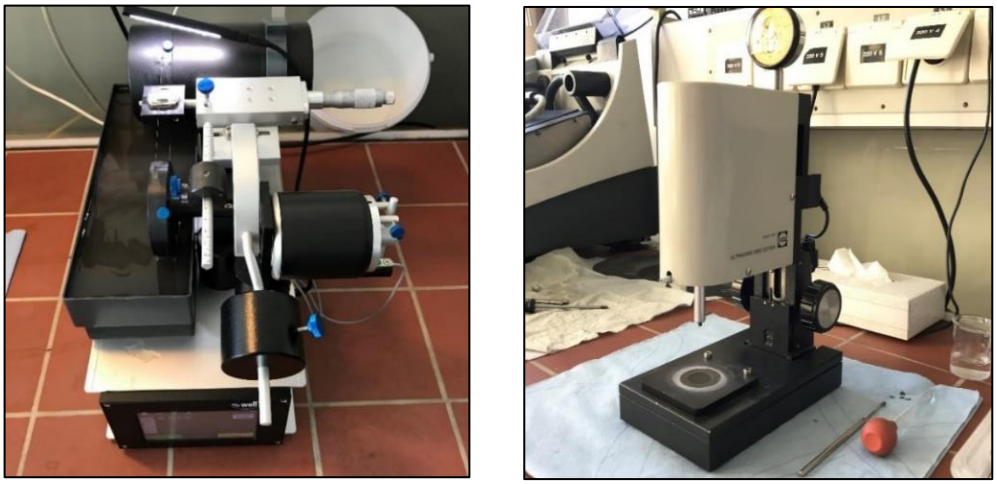

Figure 8. *a) The diamond wire saw, which is used to cut out small samples from large wafers b) Ultrasonic Cutter System.*

2.2.4.2. Mechanical grinding/polishing

Mechanical grinding/polishing uses polishing disk/lap containing different abrasive grains of decreasing size attached to a rotary system. *Figure 9.* illustrates the basic principle of the mechanical polishing procedure and *Struers'* rotary grinding/polishing machine is shown. Usually, abrasive disks are made of diamond particles, SiC, ZrC, etc. Polishing should be done in a dust-free area. Any contamination of a polishing disk/lap by abrasive particles carried over from a preceding operation or by dust, dirt, or other matter in the air should be strictly avoided. If the polishing lap becomes contaminated, without a possibility to remove all the contaminants, then it should be replaced by a clean one. Cleaning the sample from previous polishing abrasive is vital to prevent scratches on the sample and damages to the polishing disks. The specimen can be cleaned ultrasonically or carefully by swabbing with cotton using distilled water, alcohol (ethanol, isopropanol), acetone, etc.

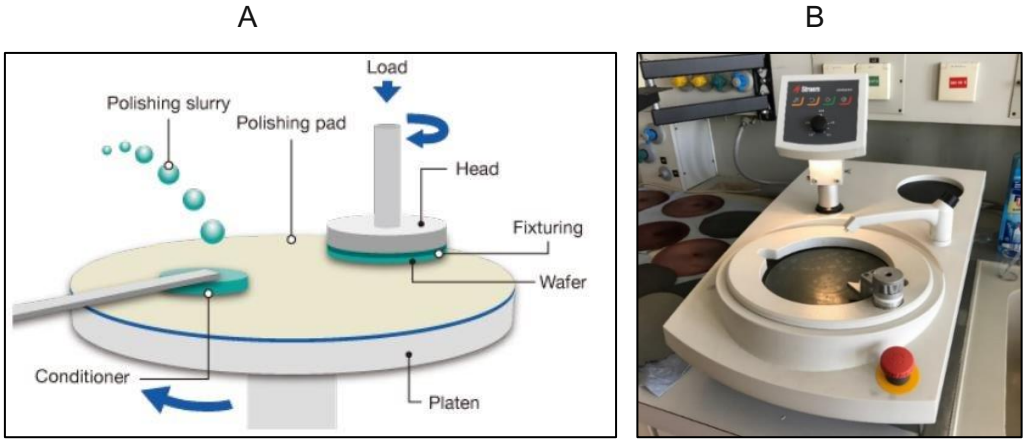

Figure 9. *a) The principle of mechanical polishing. b) Grinding/polishing machine with adjustable rotation speed (50-500 rpm) and 200 mm diameter disks available at ZONA – JKU.*

Rough polishing has the purpose of plan-view grinding and removal of the damages produced by wire cutting and/or ultrasound cutting. Plan-view grinding follows as the first step after cutting of the sample. Fixed grains with a relatively large grain size are used. It ensures maximum flatness of the sample and reduces primary thickness.

Since later in the Experimental section of the thesis, a diamond polishing abrasive is used to prepare a wedge polished sample, it will be explained in more detail here. Rough polishing is usually accomplished with diamond abrasives ranging from 9 microns down to 1-micron. Fine polishing which follows is used to remove only surface damages, i.e. polishing lines from a previously used disk/lap. It is achieved using diamond abrasion in

form of diamond paste or sprays with fine particle size (1 μm, 0.5 μm, 0.25 μm, 0.1 μm, 0.05 μm). This polishing technique can be applied to almost all bulk, compact, and thin-film materials. The parameters that must be considered during the mechanical preparation of the sample are disc surface, abrasive, grain size, lubricant, rotational directions, and speed, applied force, time, and specimen holder positioning. This allows adaptation of the polishing condition to the nature of the sample. The main disadvantages regarding possible sample destruction are mechanical damages e.g. inclusion or phase loss and cracks, thermal damage in sense of heating and fusion, and chemical damage which signifies the surface modification. [10],[60]

2.2.4.3. Dimpling and Ion Milling

Dimpling as well as mechanical polishing uses diamond paste to grind a concave imprint or dimple using a Dimple Grinder System (see Figure 10.). It involves thinning of a centre of a 3 mm disk down to 5-10 μm or less. The initial disk must be less than 100 μm thick.[61] It can be used to obtain electron-transparent surfaces much larger than if the sample had no prior dimpling. Afterward the final thinning can be performed by other preparation techniques such as electrolytic and chemical polishing or ion milling. The strain hardening for hard materials, mechanical damage of soft and ductile materials, and a thermal effect due to friction are the main disadvantages of this technique.[9] Controlling a few parameters such as the rotational speed of the specimen and the grinding wheel, quantity, and type of abrasive and lubricant, polishing time, and penetrating force, prevents mechanical damage of the sample. The thinning of the sample via dimpling reduces the required time for ion milling, especially for hard or brittle materials.

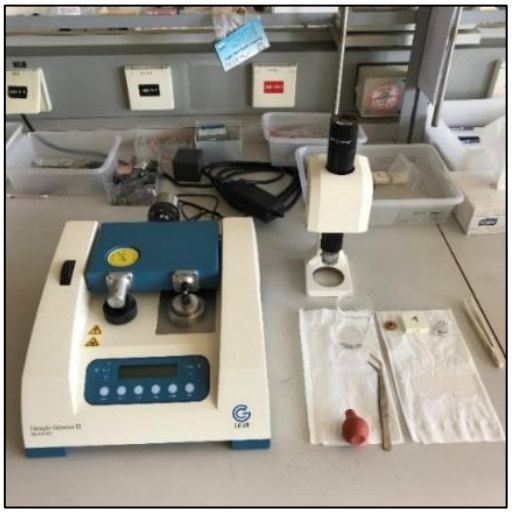

Figure 10. *Gatan Dimple Grinder System.*

Ion Milling is a physical etching technique used in sample preparation. The ions of an inert gas, usually Ar^+, are accelerated from a wide beam ion source unto the surface of a substrate in a vacuum to remove material to some desired thickness. A thin film is prepared by milling surface layer atoms with the irradiation of an argon ion beam accelerated at 2 kV to 10 kV with a grazing incidence angle of less than 10°. The continuous bombardment of the sample by ions causes damages and amorphization, thus, the ion exposure and therefore ion milling time should be minimized.

2.2.4.4. Electrolytic and Chemical Polishing

Electrolytic polishing is a technique used to achieve a bright surface regardless of the hardness of the metal or semiconductor. Besides requiring conductive material, the sample must be bulk, compact, and generally single phased. This technique is used for the removal of strain hardening caused by preliminary preparation or thinning techniques.[62], [63]
It generates almost no preparation artifacts, but it has limitations for certain multiphase materials and those containing precipitates or segregations.

Chemical polishing could be applied to all types of reactive materials. It is used to achieve surface etching with a polishing effect resulting in a flat shiny surface without bumps caused by mechanical stresses. The composition tuning of the etching solution depends on the material's chemical composition and is laborious for complex, exotic, and novel materials. The direct result of chemical polishing is microroughness smoothing.

2.2.4.5. Wedge polishing and the MultiPrep™ System

The wedge polishing is a mechanical sample preparation method. It involves polishing by rubbing a gentle abrasive on a slightly inclined sample (0.3-2°). The prepared sample is wedge-shaped with an electron-transparent edge as Figure 11. presents. The thicker side of the sample ensures easy handling of the sample. The abrasive sequence changes from coarse to finer grains to achieve a flat, evenly polished wedge. Both plan-view and cross-sectional TEM specimens can be prepared. Ion milling can be used for cleaning purposes as well. Wedge polishing can produce extremely thin sample areas with minimal surface damage. Common preparation equipment is via tripod polisher but in this Experimental work, a MultiPrep™ System will be used.

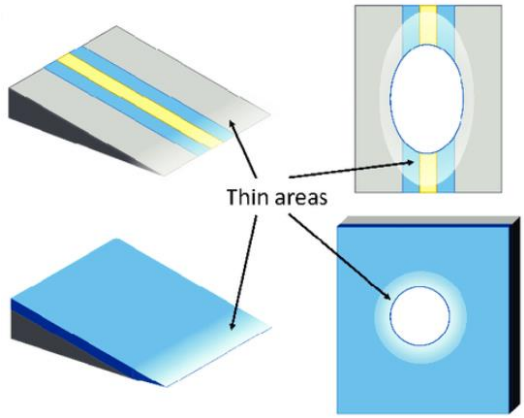

Figure 11. *Compared cross-sectional and plan-view samples prepare by wedge polishing and using dimpling and ion milling.*

The MultiPrep™ System (shown in Figure 12.) is an efficient semiautomatic tool for sample preparation for a wide range of materials for microscopic evaluation (optical, SEM, TEM, AFM, etc.). Along with parallel polishing, angle polishing, and site-specific polishing are also possible. Common applications include parallel circuit delayering, cross-sectioning, serial/3-D preparation, wedge polishing, and more. Samples are polished to electron transparency in a much shorter fashion than with the classical polishing techniques previously reviewed and often excluding the additional application of ion milling techniques.

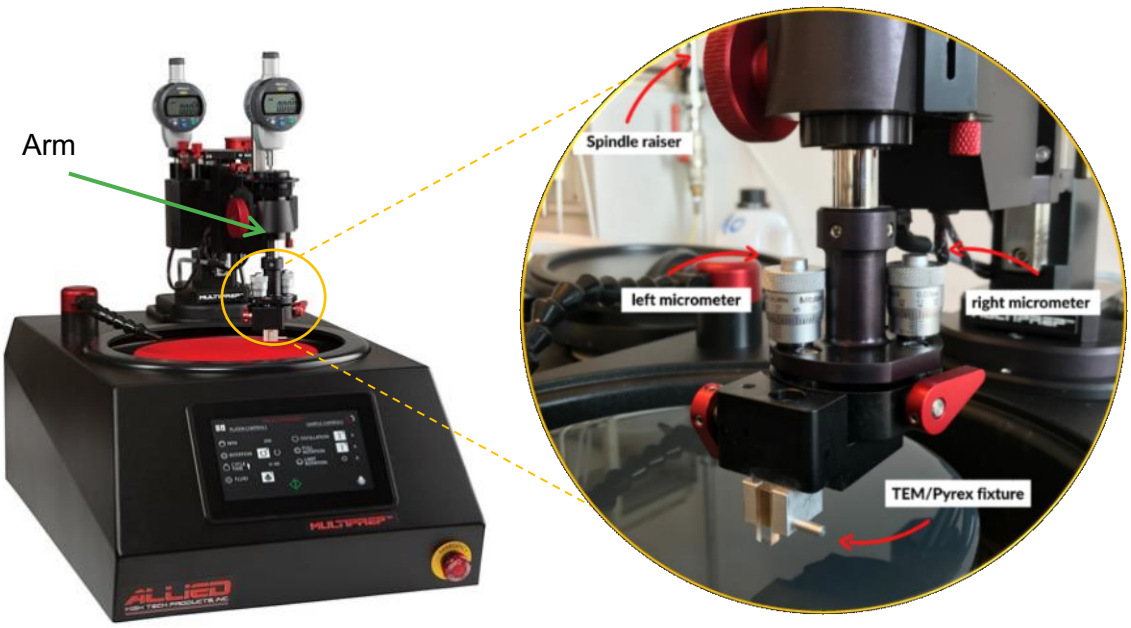

Figure 12. *Allied Tech MultiPrep System and zoom-in of some features of the instrument that are important to differentiate for wedge polishing.*

Wedge polishing or angle-lapping of materials to electron-transparency with the MultiPrep™ System allows simultaneous preparation of multiple interfaces (i.e., thin films/superconductors). The front digital indicator of the instrument displays real-time material removal. Two micrometres, axial or left (for front to back adjustment) and radial or right (for the left to right adjustment) are used to control angular positioning of the sample in step increments of 0.02°. A variable sample load can be applied to the sample, from 0 g to 500 g in 100 g increments. The instrument offers full or limited automatic sample rotation with 8 speed and variable platen speed. (5-350 RPM). MultiPrep uses Diamon Lapping Films (DLF) attached to the rotary platen. These are defined as a slurry coated microabrasive film where the abrasive grains are coated with a layer of resin which acts as bonding to the PET backing film.[64] When wedge polishing brittle materials, the thin area near the wedge tip can readily crack or cleave, leaving the remaining sample relatively thick. To avoid this, a film with fine particle sizes and slow rotational polishing speeds and low pressure must be used. Amorphization of layers reduce TEM image contrast and are it is highly undesirable. During wedge polishing, the surface becomes amorphous due to mechanical stresses. Most of these amorphous layers can be removed by grinding them away with the next finer grain size and using the colloidal silicon as the last chemical-mechanical polishing step.

2.2.5. Advanced FIB milling technique for TEM sample preparation

A focused ion beam (FIB) instrument looks and operates much like a Scanning electron microscope but instead of using an electron beam, FIB uses an ion beam to create a specimen image. FIB methods are used for imaging, milling, deposition, site-specific analysis, micromachining, and manipulation.
The dual-beam platforms, a combination of SEM and a FIB column equipped with a gas injection system (GIS) and micromanipulator serve as a method for advanced specimen preparation for TEM analysis (the dual system is presented in Figure 13.). [65] The tilt of a FIB column in such a system is usually between 52° and 55° to the vertical.[46]

The focused ion beam of metal ions is generated by a liquid metal ion source (LMIS). The LMIS contains a sharp tungsten (W) needle attached to a reservoir of gallium (Ga).[66] Ions are extracted from the LMIS to form a sharp cone and are accelerated down to the ion column up to 30 keV. Ions are focused onto the sample using electrostatic lenses. By controlling the strength of the condenser lens and adjusting aperture size, the probe current density may vary from a few picoamperes up to 60 nanoamperes. [46], [67]

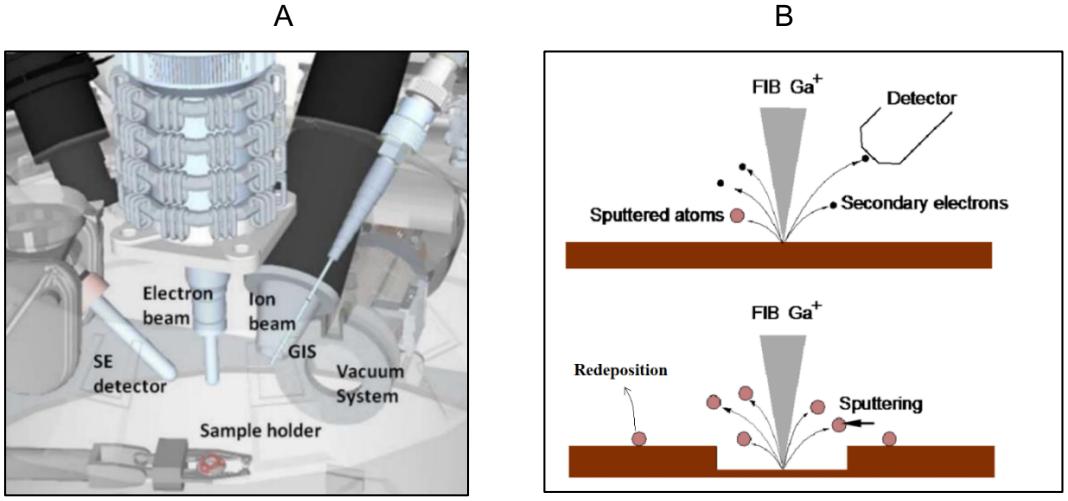

Figure 13. *a) Sample chamber of an SEM/FIB dual-beam platform [29]. b) Ion milling process using Ga^+ ions.*

When the accelerated ions hit the specimen surface, they penetrate the sample causing interactions in form of sputtering, amorphization, swelling, deposition, redeposition, implantation, and backscattering.[68],[66] Ion milling is a continuous sputtering process that can remove the material with nanoscale precision, schematically presented in Figure 13. b). That is why FIB is vital for TEM specimen preparation. Ion milling is strongly dependent

on the atomic number of materials, on the beam current, and applied voltage. FIB allows the preparation of TEM samples of hard and soft materials, regardless of how brittle, ductile, or mechanically sensitive the material is.

FIB enables the preparation of large, uniformly thick, and site-specific samples.[69] There is no other technique that can select the target area as precisely as FIB. Thus, the preparation of thin lamella is possible with a spatial accuracy of ≈20 nm.[69],[68] The preparation is usually fast, reliable, and almost independent of the nature of materials.[68]

The most common route for TEM specimen preparation is the lift out technique.

The simplified preparation procedure involves three steps: bulk milling, transfer, and thinning. A suitable area of interest of the sample is identified with SEM. In this conventional FIB technique, firstly, using the integrated gas injection system (GIS) a few tens of nanometres of a metal (e.g., Pt) or/and C capping layer are deposited on the surface to prevent implantation and surface abrasion (see Figure 14. A).[63],[65]

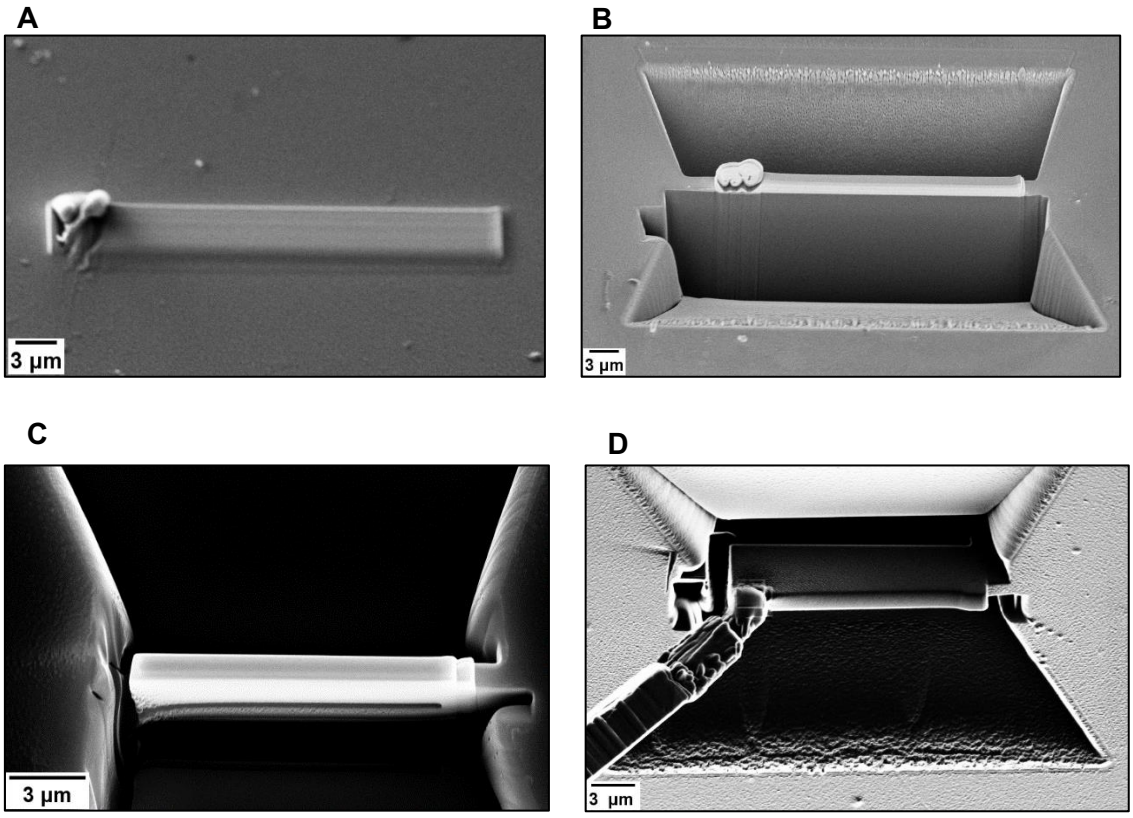

Figure 14*. Conventional cross-section TEM specimen preparation using a dual-beam tool SEM Zeiss 1540XB: a) deposition of a layer of Pt, b) two trapezoid trenches milled to a certain depth shaping a rectangular lamella, c) Ion milling sidewall connected to the bulk sample, d) Lift-out and transfer of lamella with a micromanipulator.*

Using FIB two opposing trenches are milled away as can be seen in Figure 14. B, and a 1-2 µm “pre-lamella” is made. The next step involves cutting the bottom part and the side trench away (see Figure 14. C) until the sectioned pre-lamella is attached to the bulk sample only by one side. The stage with the sample is tilted about 5° to 10° so that the beam can directly access the lateral surface of the lamella to make an undercut as presented in Figure 14. C). The micromanipulator is brought closer to the pre-lamella and welded to it using ion-beam assisted platinum deposition as it is presented in Figure 14. D). The remaining connection to the bulk sample is milled away and the lamella can be lifted out from the sample. The next step is the transfer of lamella and welding to a TEM grid as Figure 15. a) and b) shows. FIB lift-out TEM grids have been designed to attach/weld the TEM lamella milled out by SEM/FIB or FIB systems.

Thinning to electron transparency can be observed via the SE detector of the SEM. This is an important feature since it allows better control of the milling process i.e. if the lamella is about to get cutaway or any other unwanted changes are visible, milling can be interrupted manually. When the sample is thin enough, it will appear brighter in the SEM image as it is presented in Figure 15. a).

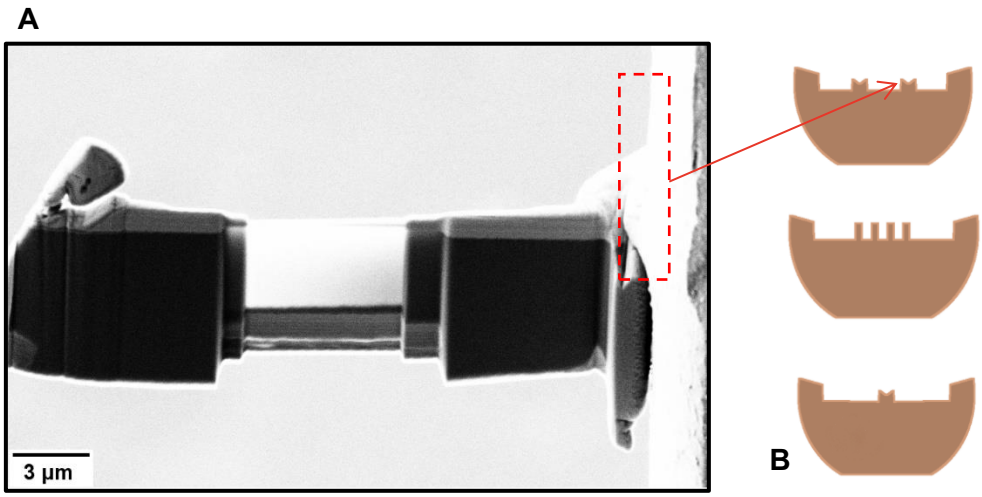

Figure 15. a) Final thinning of the TEM lamella welded to a half grid. b) Different types of half-grids.

FIB very applicable to cross-sectional lamella preparation and less suitable for plan-view preparation. The plan-view preparation can be improved by combining it with the wedge polishing technique. In the frame of this thesis, this approach was used in the sample preparation procedure as well. A Plan-view sample must be prepared to preserve the epitaxial layers of $Ge_{1-x}Sn_x$ and investigate its morphology. The detailed preparation process will be further described in the Experimental Chapter.

The main disadvantage of FIB is related to the nature of the milling process as it relies on the physical sputtering of the target.[70],[71] Sputtering removal initiated by ion collision during the bombardment of the material with Ga^+ ions can lead to ion implantation and cause damages in the sample. Induced artifacts during FIB milling are dependent on the beam current, the angle of incidence, the temperature of the specimen, and the accelerating voltage.[65], [66] Radiation damage leads to several morphological impacts causing changes in intrinsic physical properties (crystallinity, elasticity, charging of the sample, conductivity), and chemical characteristics of the surface (hydrophilicity, surface composition).[69]

2.2.6. Micro-Electro-Mechanical Systems (MEMS)

Micro-Electro-Mechanical Systems (MEMS) are mechanical sensors and actuators that are fabricated using techniques like those used for integrated circuits.[72] MEMS are micrometre-sized mechanical structures (see Figure 16. A) that can receive information from their environment. MEMS-heating chips usually consist of a free-standing membrane of silicon nitride with an embedded element surrounding the contact point and electron transparent windows or through-hole (see Figure 16. b)).[73] The element has a spiral configuration, and the membrane is heated by the Joule first law[1] i.e. when the current is passing through the heating element.
It can also respond to signals of the control system to change the environment. The design of the MEMS heating chip and its controller assure temperature stability within 1°C after only a few tens of milliseconds from the starting heating temperature. Very low heating power of several mW has no impact on the detection of any SEM/FIB signals (SE, BSE). MEMS chips can be reheated several times without the loss of performance.

[1] Joule's first law shows the relation between heat generated by an electrical current flowing through a conductor ($Q=I^2 \cdot R \cdot t$; where Q is the amount of heat, I is the current, R is the electrical resistnace present in the conductor, and t is the time.

Improvement of *in situ* TEM experiments is improved by combining site-specific sample preparation using SEM/FIB and *in situ* heating solutions kits (heating holder and heating chip).[72],[55]

The MEMS-based heating chip and the heating holders are the current states of the art method to carry out annealing TEM experiments.[74] The heating holder has a 4-point probe connected to the nanochip providing accurate control during heating with 0.005°C stability.[75] The main advantages of a MEMS-based heating holder are reduced thermal inertia and the direct contact between the specimen and the heated membrane.[72]
The main evident drawback of the MEMS-based heating holder is the decreased quality of EDXS measurements due to the infrared radiation of the heating spiral at temperatures above approximately 750°C. In the experimental work of the thesis, DENSSolutions Wildfire heating holder (Figure 16. A) and a MEMS-based chip are used.

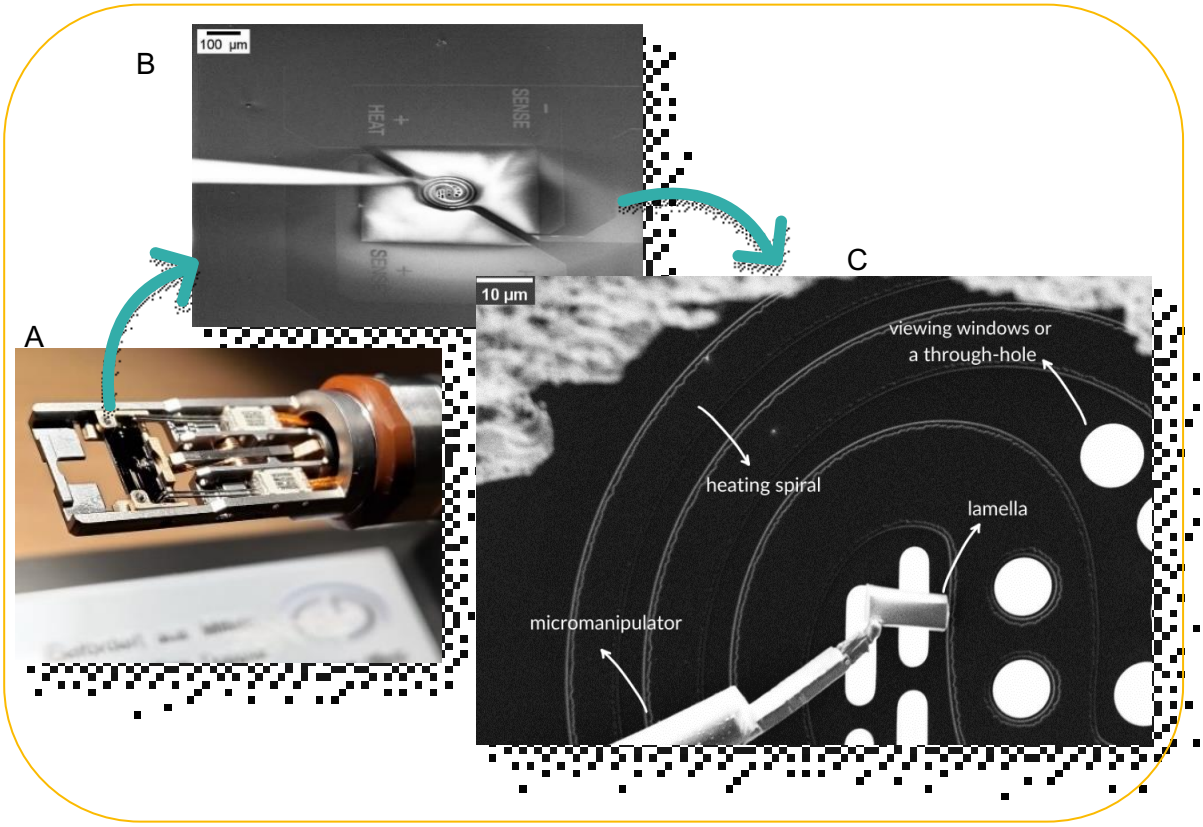

Figure 16. *a) In situ heating sample holder for Transmission electron microscope investigation with installed MEMS-based chip [Christian Doppler Laboratory for Nanoscale Phase transformations]. b) SEM image of the MEMS-based heating device c) FIB image of MEMS-based chip during the in situ transfer of a lamella.*

2.2.7. Atomic force microscopy

The atomic force microscope (AFM) is a type of scanning probe microscope. A typical AFM consists of a cantilever with a small tip (probe) at the free end, a laser, a 4-quadrant photodiode, and a scanner.[77],[78] The working principle of an AFM is based on the cantilever/tip probe that interacts with the sample in a raster scanning motion. AFM uses a laser beam deflection system to gain topographical information of the surface. The laser is reflected from the back of the reflective tip onto a position-sensitive detector.

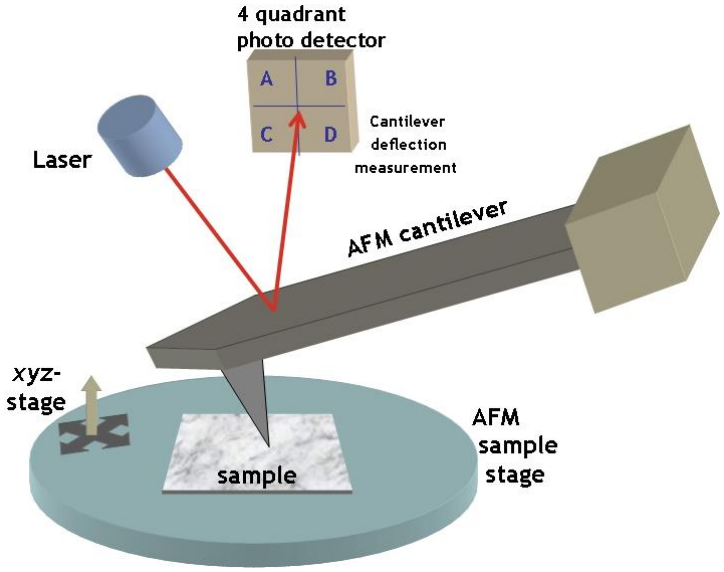

***Figure 17**. Scheme of a basic working principle for an AFM. The deflection of the cantilever produced by the tip-surface interaction changes the incidence of the laser onto the photodiode detector.*

This technique provides a 3D profile of the surface at the nanoscale by measuring forces between sharp probe, with a radius from few up to 10 nm, and surface at very short distances (0.2-10 nm). These forces are dependent on the spring constant or stiffness of the cantilever and the distance between the probe and the surface. The force can be described using Hooke's Law: $F = -k \cdot x$, where F is force, k is spring constant and x is cantilever deflections. [76]

The motion of the probe across the sample is controlled using a feedback loop and piezoelectric scanners. The probe generally does not move, while the sample is moved in the x,y,z direction by a piezo-actuators (ceramic that can expand or shrink when a voltage is applied). The measured interaction in short probe-sample distances is Van der Waals (VdW) interaction. Meanwhile, capillary forces, electrostatic and magnetic interactions are more significant in long-range interaction.[76] The AFM has the advantage of imaging almost any type of surface, including polymers, ceramics, composites, glass, and biological samples. It provides nanoscale information on surface roughness. AFM imaging is useful in the sample preparation process. The prechecking of the sample with AFM provides nanoscale morphological information, where scratches, impurities such as dust particles, or remaining of the cleaning solution can be easily distinguished.

AFM non-contact mode has been used to pre-check the MBE samples. In this mode, the AFM system detects changes in the resonant frequency or vibration amplitude as the tip comes near the sample surface. The system vibrates a stiff cantilever near its resonant frequency (typically 100–400 kHz) with an amplitude of a few tens to hundreds of Angstroms.

3. Experimental Approaches and Results

This Chapter will provide characterization measurements of the MBE grown samples and the sample preparation procedure for the installation of $Ge_{1-x}Sn_x$ sample onto a MEMS-based heating chip. Each step contributing to a successful *in situ* TEM heating experiments will be in detail described. This includes the sample preparation protocol that was developed, the step-by-step preparation of MEMS-based heating chip with GeSn specimen, and Si sample with Ge quantum dots as reference material.

3.1. Challenges in TEM sample preparation procedure

As it was previously pointed out, the sample preparation procedure is an essential step in the investigation of materials with TEM. The goal of the Experimental work is to develop a suitable and easy-to-follow sample preparation method to investigate the epitaxial layer of $Ge_{1-x}Sn_x$ alloy.

Conventional preparation methods were previously reviewed in Section 2.2.5. and are more suitable for cross-sectional samples. Here wedge polishing technique was used to prepare a plan-view sample of $Ge_{1-x}Sn_x$ and Si with quantum dots as reference material.

The wedge polishing technique is a common method usually performed using a tripod polisher or more advanced semiautomatic or automatic devices. The mechanical wedge polishing of Si with Ge quantum dots (QDs) and $Ge_{1-x}Sn_x$ samples in a frame of the master's thesis has been carried out with Allied Tech MultiPrep™. One of the main challenges regarding the wedge polishing technique is the determination of the sample's thickness.

The monitoring of the thickness during the process with a precision of a few micrometres is difficult, but it is crucial to obtain a damage-free surface. In practice, while downsizing the sample to electron transparency, the polishing material having finer and finer particle size should be used in the polishing procedure. Therefore, knowing accurately the thickness of the sample we can change polishing abrasives at the proper thickness. For instance, 15 μm polishing material should not be used if a sample is 20 μm thick. This can introduce unwanted artifacts on the surface i.e. scratches, delayering, roughness, and the sample will most likely be damaged and may even break. While proceeding with the wedge polishing, the thickness can be determined using a thickness gauge (accuracy up to 1 μm), and a VLM (gradation lines or transmission of light through the sample). Difficulties related to the monitoring of the thickness can be bypass with Si/Si-based samples. Hence the procedure for wedge sample was firstly tested with Si. The colors of Silicon viewed in a transmission VLM mode have been used for many years as a technique for monitoring the thickness of the silicon sample during the preparation process. Observations of the Si samples showed

that 5 to 10 μm thick Si samples have a deep red color. Further thinning leads to a light yellow color when the thickness reaches approximately 1 μm. Si sample becomes colorless if the thickness is less than 1 μm. Another related qualitative thickness-monitoring technique is the observation of the appearance of optical interference fringes of thinned silicon samples. The interference fringes are a result of constructive and destructive interference between transmitted light and light that has undergone multiple internal reflections and can be seen in the thin area of the sample by a VLM. Interference fringes appear in the sample is less than 1 μm thick. To simplify thickness determination during the development of the sample preparation procedure Si sample was used as reference material.

FIB techniques are ordinarily applied to samples that can be cross-sectioned. Nonetheless, FIB is less suited to plan-view sample preparation which is particularly important in the characterization of the morphological features of a thin film. To pursue *in situ* heating experiment in TEM, the FIB sample preparation technique is combined with wedge polishing preparation to prepare plan-view electron transparent lamella.
The wedge-shaped thinning to approximately 2-3 μm or even up to electron transparency shortens the ion milling time and thus less damage is caused in the sample by ions.

3.2. Sample Description and Characterization

The samples tested for the wedge polishing procedure were synthesized by MBE at the Institute of Semiconductors and Solid State Physics of the Johannes Kepler University Linz. To characterize the quality of MBE samples from *Table 2.*, AFM and XRD (*X-Ray Diffraction*) were used.

Table 2. *Overview of the MBE samples that were used for the elaboration of the sample preparation procedure.*

Labelling	***Specification***	***x → ($Ge_{1-x}Sn_x$)***
4692_BASG	Si with Ge quantum dots (QD)	-
4881_BAVGT	GeSn active layer (50 nm nominally) grown on Ge buffer (50 nm nominally)	x_{center} = 0.0456 x_{side} = 0.0449
4884_BAVGT	GeSn active layer (50 nm nominally (grown on Ge buffer (50 nm nominally)	x_{center} = 0.1041 x_{side} = 0.1059

Prechecking of the sample with AFM was performed in non-contact mode *Gwyddion 2.59* software was used for processing images. This is a software used in Scanning Probe Microscopy (SPM) data visualization and analysis. It can be used for general height field (greyscale) and image processing.

Using Gwyddion software, Roughness parameters were calculated and presented as graphical data. To gain more information on the topography and render the roughness information more accurately, 3-dimensional AFM image conversion is advantageous. The AFM images were obtained using 0.3 scan lines per second and 512 points per line mode.

3.2.1. Si with Ge quantum dots

To solve sample preparation challenges a simpler model system was used. An MBE Si sample with free-standing Ge QDs that are randomly distributed across the Si surface is presented in Figure 18. The Ge QDs are approximately 0.84 nm high. A scheme of MBE grown Si sample is presented in Figure 18. a). Si (100) was used as a substrate on which a Si-buffer was grown. Ge QDs are epitaxially grown on a clean Si buffer. Figure 18. depicts the images obtained with non-contact mode AFM and represents the surface of the Si sample where Ge QDs can be spotted in the topography image and the 3D reconstruction.

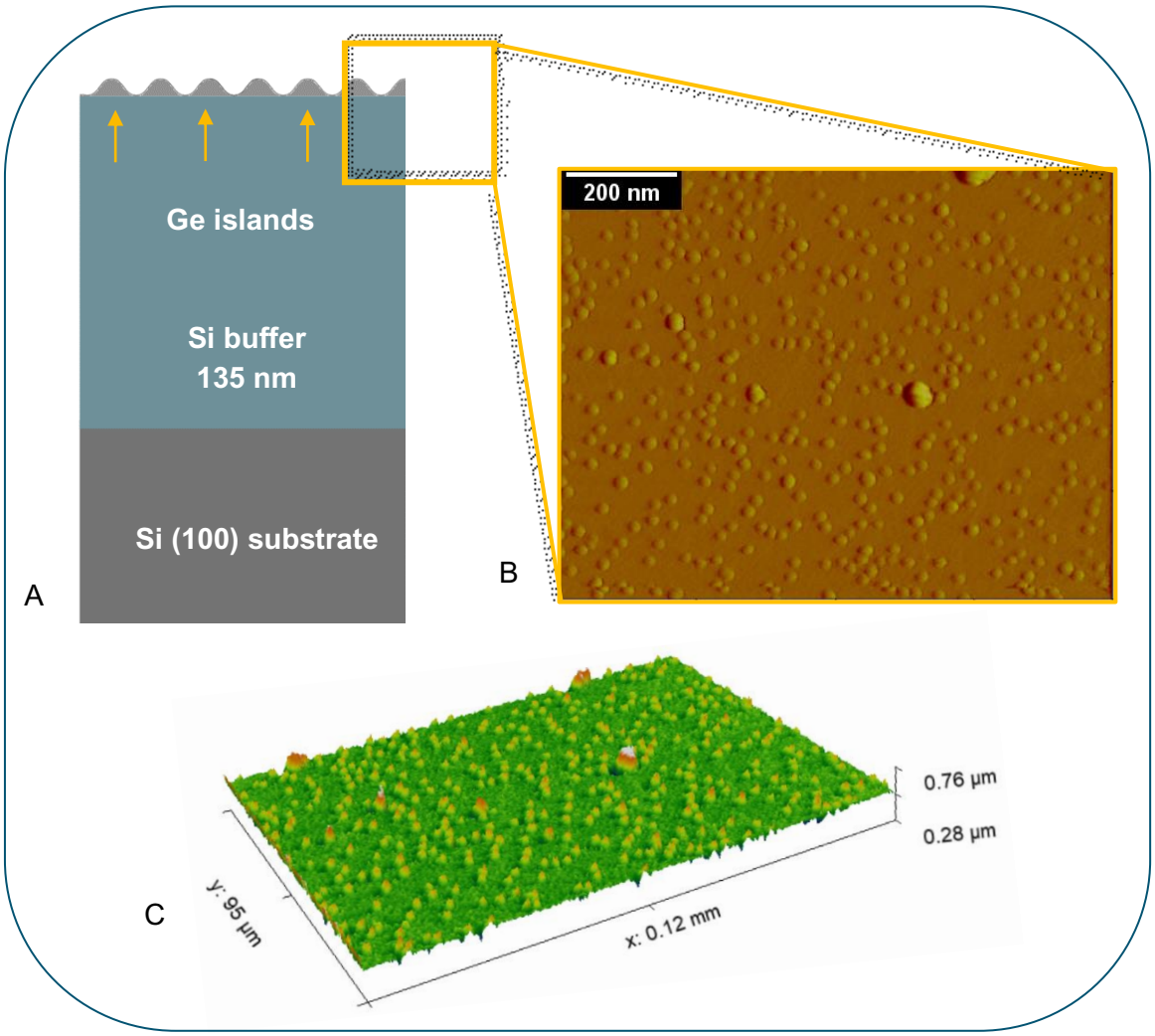

Figure 18. *a) The scheme of the Si sample with Ge QDs b) AFM measurement Si sample with Ge quantum and c) Gwyddion 3D simulation.*

3.2.2. $Ge_{1-x}Sn_x$ Samples

The schematic of the layer structure of the MBE $Ge_{1-x}Sn_x$ sample along with the TEM image is presented in Figure 19. As can be seen on top of Ge (001) substrate a ~50 nm thick Ge buffer is grown. The $Ge_{1-x}Sn_x$ grown on top of Ge buffer is 50 nm thick as well. Here the model of the $Ge_{1-x}Sn_x$ sample is correlated to the TEM image of the cross-sectional prepared sample. In the Figure interfaces between substrate-buffer and buffer-layer can be distinguished.

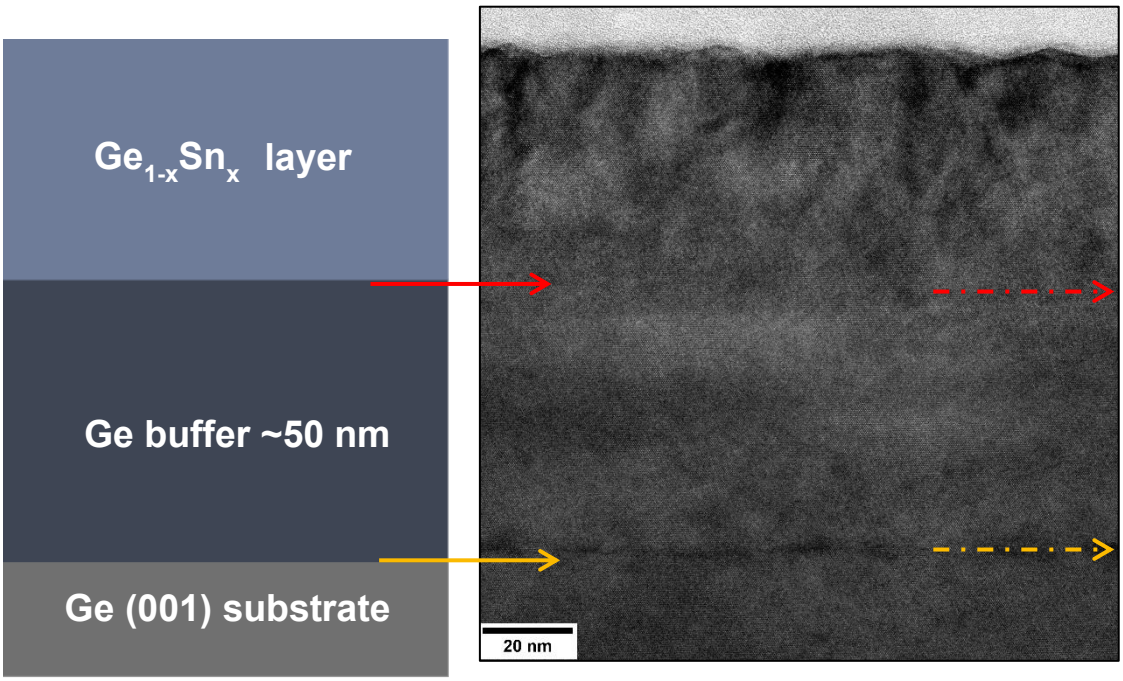

Figure 19. *The scheme of the MBE Ge-Sn samples and high-resolution TEM image.*

Further characterization was done by AFM measurements and explained through a set of topography data. Figure 20. demonstrates the AFM measurement of a representative $Ge_{1-x}Sn_x$ sample from the series with **4,5%** of Sn content. Widely smooth and even surface is present with negligible height differences. Besides pristine surface regions, many sites exhibit rather deep holes presented as dark spots in the topography image in Figure 20. The presence of deep holes is related to the cleaning procedure during the growth of the material. It is not possible to accurately represent and determine the depth of the pores with AFM. Formed 3D surface topography shows a uniform and quite even surface.

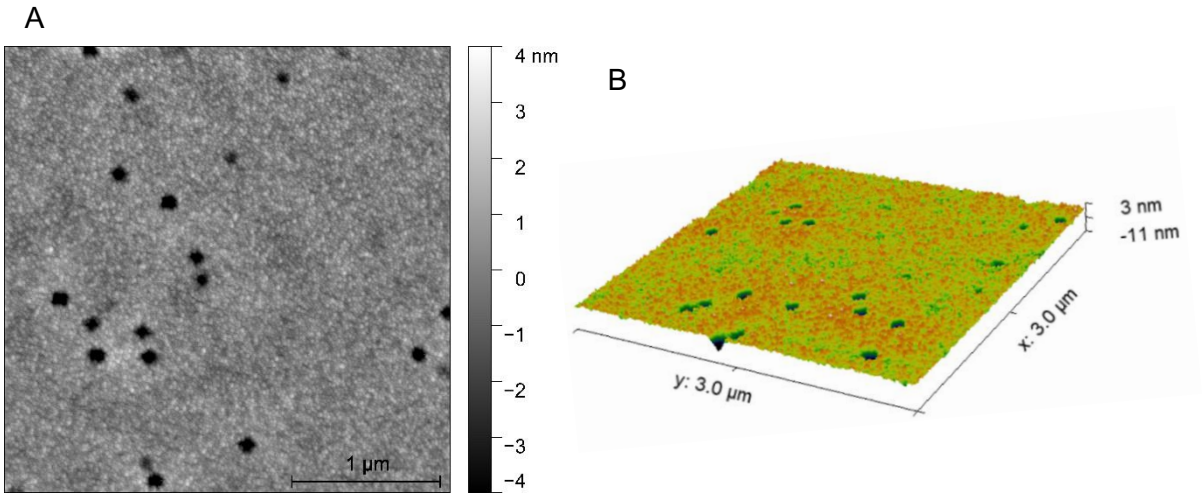

Figure 20. *AFM non-contact mode measurements; a) topography image of Ge-Sn (4.5%) sample, b) 3D simulation of surface.*

No-droplet formation on the surface is observed. The growth temperature is 150 °C which is below the eutectic temperature of $Ge_{1-x}Sn_x$ binary alloys (231.1 ◦C). This can efficiently restrain the Sn surface segregation.

The MBE $Ge_{1-x}Sn_x$ sample with *10.56%* of Sn content is quite relevant since the direct bandgap of Ge can be achieved with Sn concentration above 9%. Figure 21. presents the AFM measurements. From the topography image, the surface is uniform and defects free. Holes-like structures that are deeper in profile than the rest of the surface are also observable as dark-colored regions. Compared to the previously tested sample, this surface seems rougher as can be seen in the colorized 3D topography as well. AFM image shows no-droplet formation of Sn precipitates on the surface.

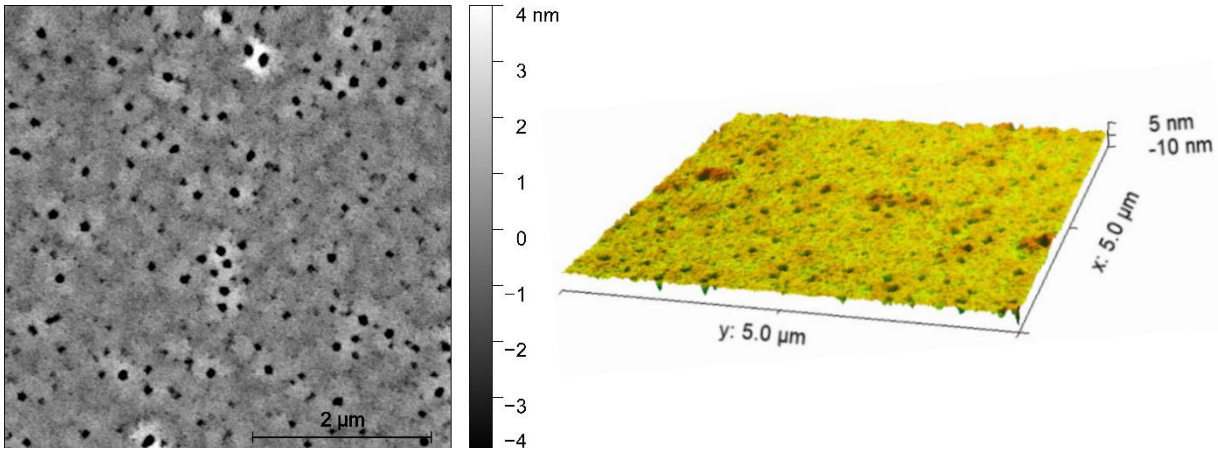

Figure 21. *AFM non-contact mode measurements; a) topography image of Ge-Sn (x=10.56%) sample, b) 3D simulation of the sample's surface.*

3.2.3. XRD Measurements

The XRD measurements were performed by an MBE growing group and are presented in this thesis to show the quality of synthesized samples. XRD is a non-destructive technique for characterizing a crystallographic structure of materials. It could also provide detailed information on the chemical composition and physical properties of materials. XRD peaks are produced by constructive interference of a monochromatic beam of X-rays scattered at specific angles from each set of lattice planes in a sample. Consequently, the peak intensities are determined by the atomic positions within the lattice planes. The result is a plot of diffracted intensity (counts) vs. angle. The XRD measurement gives valuable information that can be used to improve the growth method of the samples. In Figure 22. the XRD measurement for $Ge_{1-x}Sn_x$ samples with x=4.5% and x=10.56% are presented. The reference pattern shown as the orange line ("fit") is a result of computer simulation of the structure. The position and intensity of the fit line should match the measurement data. An amount of mismatch in peak position and intensity is an acceptable experimental error. XRD can be also used to measure the thickness of thin films. Interference fringes observed in the scattering pattern are caused by different optical paths of the X-rays and related to the thickness of the layers. Measurement curve coincides with calculated and simulated data which confirms that the heteroepitaxial $Ge_{1-x}Sn_x$ layer has high crystalline quality and is coherent with the Ge substrate.

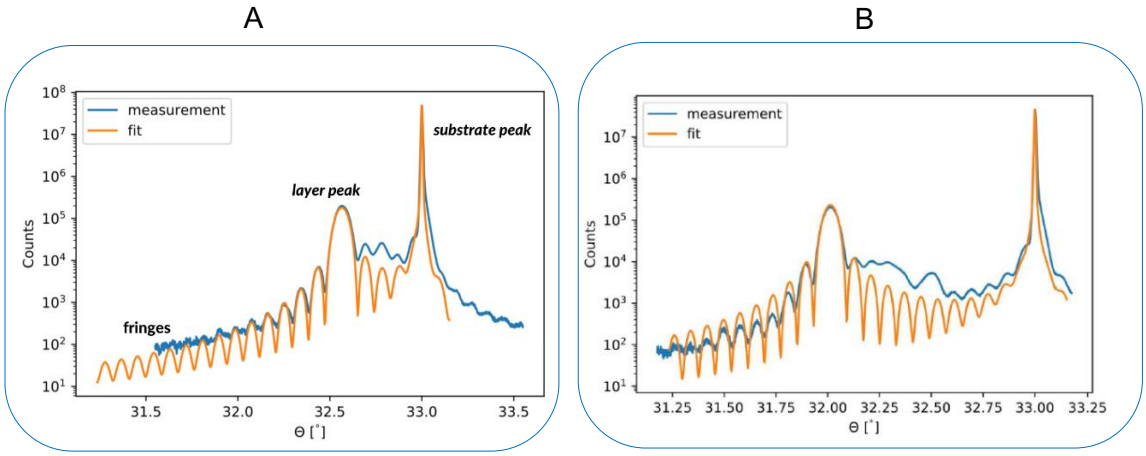

Figure 22. *XRD graph of experimental ω/2θ (blue) and simulated curve (orange) for* $Ge_{1-x}Sn_x$ *sample with x=4.5% (A) and x=10.56% (B).*

3.3. Elaborated Wedge Polishing Procedure

Few preliminary steps must be carried out to successfully prepare an electron transparent wedge polished sample. One of the preliminary steps is polishing the TEM/Pyrex paddle used for mounting the sample. The TEM/Pyrex paddle must be polished parallel to the abrasive plane to establish a reference surface. Therefore, Pyrex is attached to the cam-lock adapter of the MultiPrep System, and first, a flat surface was achieved using the 9 or 6 μm Diamond Lapping film (DLF). In this step, any deformation (small rupture) or unevenness of Pyrex glass can be removed. Using smaller sized DLF, up to 0.1 μm, a parallel, flat polished reference is established. This drastically facilitates the thinning of the sample parallel to the edge of the Pyrex. Furthermore, if the Pyrex is polished in this way only the adhesive used to secure the sample to Pyrex can interfere during polishing. But if the sample is glued properly these effects are negligible. *Figure 23.* shows the summarized sequence of steps required to prepare the wedge polished sample.

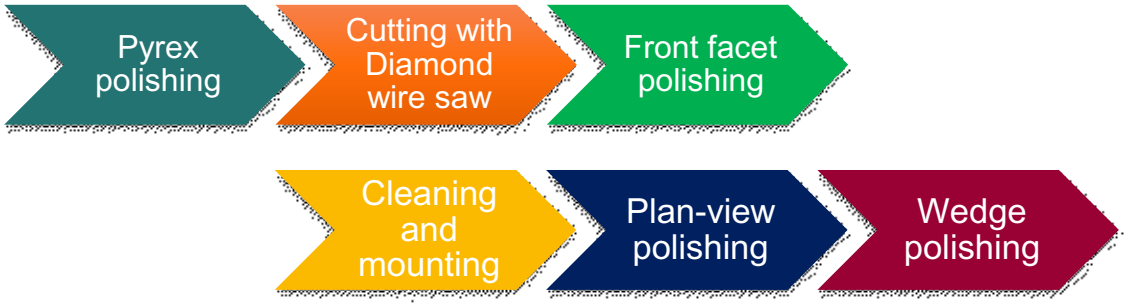

Figure 23. *Steps in the procedure for mechanical wedge polishing.*

WELL Diamond wire saw is used for cutting the sample into a rectangular shaped one with dimensions of 2.5 mm x 1.6 mm (the thickness of the diamond wire is ≈40 μm). Afterward, the sample is cleaned in the Ultrasonic cleaner for 1-3 minutes with various chemicals and cleaning solutions. First, acetone (Ac) is introduced to remove wax stains and remaining. Ethanol (EtOH) or Isopropanol (IPA) can be used to remove acetone stains from the surface. Distilled water is used in the Ultrasonic cleaner to remove EtOH.

As Figure 23. is suggesting, the next step is to polish the lateral front face of the sample. This is one of the crucial steps. Mounting the sample could be done using either wax or glue (super glue), and both are dissolvable in Ac. Both wax and super glue were tested, but any noticeable differences have not been observed during polishing. Curing time of wax bond is short (5-10 minutes), meanwhile, super glue requires ≈20-30 minutes. Therefore, Allied Tech Mounting Wax was used in the entire procedure. Mounting is done in a way that the front facet is pushed further from the edge of the Pyrex (≈2-3 mm) as Figure 24. shows. The

surface of interest in glued face-down to the Pyrex so it can stay protected during polishing. This step produces an even surface of the front facet. To avoid cracking and unwanted delayering of the surface of interest and polished surface during plane polishing or wedge polishing the front edge of the sample must be finely polished. Further polishing involves the application of 3 µm, 1 µm, and final fine polishing with 0.5 µm and 0.1 µm DFL. The sample is then unglued from the Pyrex, cleaned with Ac, EtOH/ISP, Micro organic soap (Allied Tech), and distilled H_2O.

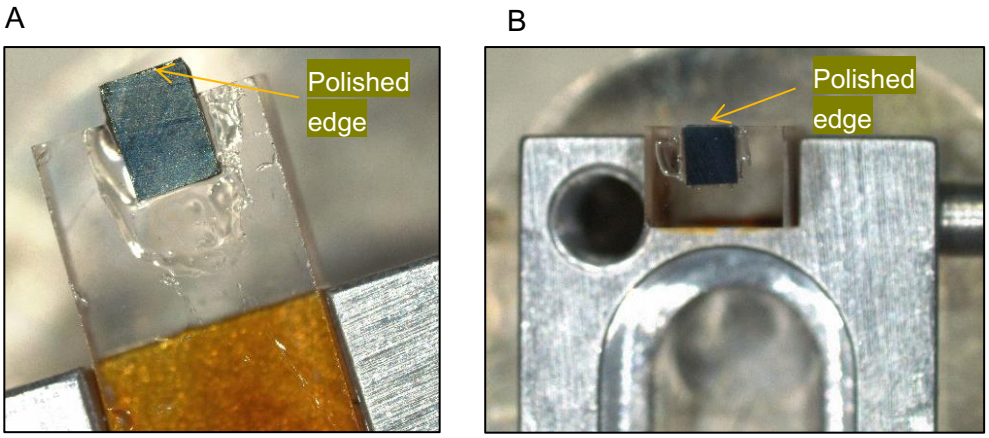

Figure 24. *VLM images of a) position of the sample for the front edge polishing and b) position of the sample for the plane and wedge polishing.*

Now it is possible to proceed with the wedge polishing procedure. The overall procedure is divided into two main steps: thinning the sample to approximately 200-150 µm (plane polishing/grinding) and the introduction of an angle to the polishing procedure.

The surface of interest is directly glued to the Pyrex holder. The TEM/Pyrex and a microscope slide are heated on a hot plate set to 100-150°C. A small amount of wax is melted on the slide. The sample is lifted with tweezers and the surface of interest is placed into the wax. Afterward, the sample is lifted and placed on the clean surface of the glass slide for about 10 seconds to allow the wax to flow from the sides of the sample. This step is repeated several times to remove excess wax. The sample is lifted and placed onto the Pyrex. Using the end of a toothpick or any other applicator with firm but gentle pressure, the sample is pressed against the Pyrex to squeeze the excess of glue and produce a thin glue layer. The positioning of the sample close as possible to the front edge of the Pyrex, as images B in Figure 24. And Figure 25. depicts, is done using the end of a toothpick and it can be observed with a stereomicroscope. The Pyrex with the mounted sample should be left for 10 minutes at room temperature to allow the wax to solidify.

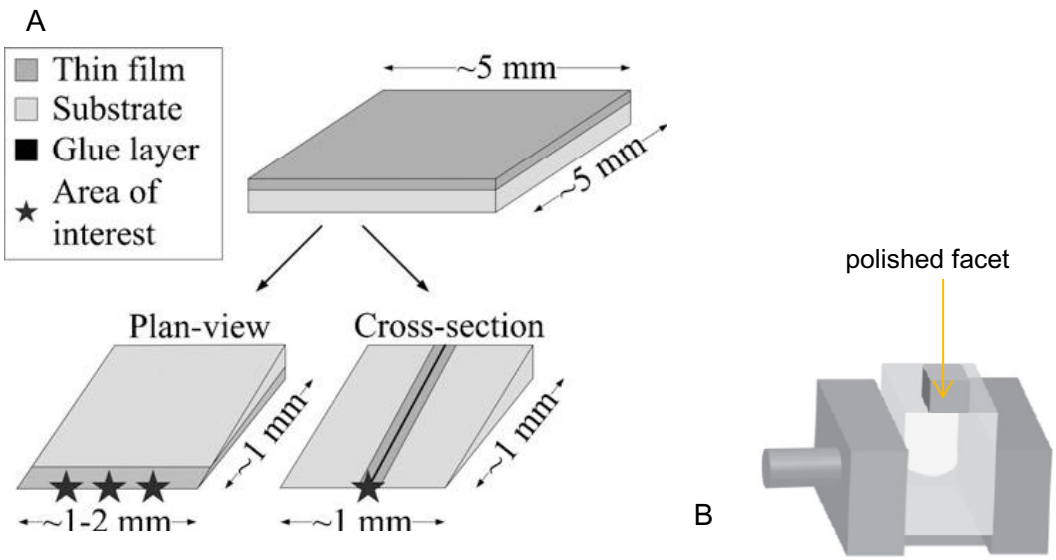

Figure 25. *a) Schematic representation for wedge polishing sample where an electron transparent edge is achieved in interest. b) Sample position versus Pyrex glass for wedge polishing.*

The height of the sample versus the rotation plate can be controlled by two features of the MultiPrep. The spindle riser located on the left side of the arm is used to raise or lower the spindle/sample without changing the vertical position of the arm (please see Figure 12. MultiPrep System). Meanwhile, the vertical adjustment knob is used to control the vertical position of the sample as defined by the arm assembly, so it is used to lower/raise the sample by a counterclockwise/clockwise rotation.

Before proceeding with the polishing, the starting thickness of the sample can be determined with a thickness gauge. The starting thickness of the Si sample is 520 μm (it can vary). The 6 μm DFL is secured to the platen and the Pyrex paddle is attached to the MultiPrep. The load is set to a maximum (500 grams). The sample is positioned on the rotary plate so when the oscillation is activated the sample is moving between the edge and the centre of the platen. The arm of the MultiPrep is raised more than the thickness of the sample so when the spindle riser is lowered the sample does not touch the plate with the attached DFL. The sample is lowered with the vertical knob until it makes full contact with the platen. The front dial indicator is set to zero. With the vertical adjustment knob, the sample is lowered into the DLF until a trail of removed material is observed and the dial indicator is displaying 1-5 microns. The platen rotation is activated in a counterclockwise direction at 25 RPM and the oscillation is set to be lowest. Coolant (water) and lubricant (*BlueLube – Allied Tech*) are applied onto the DLF. In general, the lubricants are used to achieve the highest possible removal rate, finest surface finish, and minimize the effects of friction. The *BlueLube* is a denatured alcohol-based lubricant and cooling agent with low

viscosity, it enhances the polishing performance and helps in maintaining the durability of the polishing cloth.

Using a vertical adjustment knob, the sample is gently lowered into the abrasive. The dial indicator should display 1 μm when the sample makes full contact with the abrasive.

The platen rotation is increased to 35 RPM. The Si sample is thinned to ~350 μm using 6 μm DFL. The sample is regularly checked under an optical microscope to observe the quality of the polishing and catch sight of produced artifact or impurities. Before VLM checking and between different DLF the sample is cleaned with ethanol and water then dried using a compressed air gun. If any sturdy stacks of dirt are present, they can be removed using a cotton swab dipped in acetone or Microorganic Soap. Although, acetone should be avoided at any time possible because it dissolves wax.

Further polishing proceeds with 3 μm DFL to ~250-200 μm. Once again, the sample is withdrawn using a spindle riser and is removed to measure the thickness and clean the polished surface. The 1 μm DFL is secured to the plate and further removal is done until approaching thickness of ~150 μm. The sample must be observed under VLM to inspect the polished surface and the quality of the glue line. Cleaning with a cotton swab can leave cotton fibres which must be removed and during the whole procedure the glue support must be retained. The front edge of the sample must be perfectly cleaned before proceeding with wedge polishing. With 1 μm DFL attached an inclination angle is introduced to the polishing procedure. Rotating the vertical adjustment knob, the arm is raised at least 4-5 full rotations because the angle adjustment will drive the front edge of the Pyrex holder closer to the platen. Rotating clockwise the front “left” micrometre the desired angle is set. The scale graduation is manufactured so that each increment adjustment creates a 0.02-degree angle on the sample. Fifty lines, therefore, equals a full rotation and an angle of 1°. For hard and brittle materials (such as Si) the higher angle should be used but not too steep so that every level of material can be thinned from top to bottom. Inclined polishing was tested with 1° and 2° angle and both are giving equal results. The angle polishing can be observed by the presence of a polishing line as the material is polished at an angle. The polishing with 1 μm DFL is stopped at approximately 100-80 μm and further polishing up to 10 μm is done using 0.5 μm DFL. Thickness with thickness gauge can be measured with an accuracy of up to 1 μm. Thinning to electron transparency is achieved with 0.1 μm DFL. The polishing line on the surface might be still visible at this point. It is known that particles of a specific size can cause scratches into the sample 3 times deeper than their size. Therefore, constant VLM checking and thickness determination guide to correct exchange of DLF. Polishing with 0.1 μm can be stopped if the Si sample appears white or if the color fringes are visible as Figure 27. shows. With OP-U standard colloidal silica suspension for final polishing with a particle size of 0.04 μm the polishing lines can be eliminated. The OP-U colloidal silica suspension

is quite difficult to clean. It needs immediate splashing with acetone and intense cleaning with a cotton swab which sometimes could break the thin sample. Also, the cloth used for OP-U polishing is soft and the Pyrex with the sample is not smoothly moved across the cloth, hence this step should be carefully performed. A more suitable option is the Allied Tech Red C Final polishing cloth which as well removes any polishing artifacts.

Difficulties in achieving a sufficiently thin electron transparent wedge of the sample are correlated to the inability to precisely determine thickness. Pyrex glass allows the transmission of light and the thickness of Si can be determined by color appearance. Color-thickness dependence is presented in Table 3.

Table 3. *Dependence of thickness and color presence in Si and Si-based samples.*

Thickness	Color
~ 5-10 µm	Dark red
~ 1 µm	Light yellow
less than 1 µm	colorless
less than 400 nm	interference fringes appear

The procedure used for the Si sample is applied to the **$Ge_{1-x}Sn_x$** samples. The wedge polishing procedure for the $Ge_{1-x}Sn_x$ sample is way more challenging. One of the main challenges is that the $Ge_{1-x}Sn_x$ sample shows no color changes during thinning. The thickness related problem was overcome by polishing $Ge_{1-x}Sn_x$ samples along with Si sample as Figure 26. presents. In this way, the $Ge_{1-x}Sn_x$ thickness can be at least approximately defined by the color presence of the Si sample.

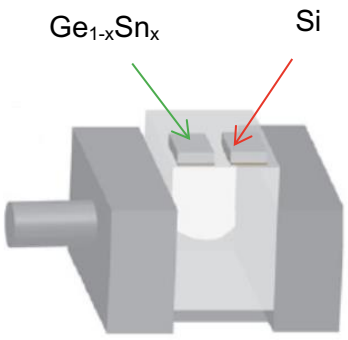

Figure 26. $Ge_{1-x}Sn_x$ *sample polishing alongside with Si sample to determine thickness according to Si color changes.*

Another obstacle in the sample preparation procedure is the metastable 50 nm epitaxial $Ge_{1-x}Sn_x$ layer. As high temperature and eventual strain relaxation promote Sn segregation any heating must be avoided to preserve the original surface of the material. When mounting the sample wax should not be heated more than 150°C. After positioning the sample on Pyrex, the holder with the mounted sample should be removed immediately from the heating plate. The $Ge_{1-x}Sn_x$ sample after front facet polishing is mounted on the Pyrex along with Si. The initial thickness for $Ge_{1-x}Sn_x$ samples is between 460 and 520 µm. The polishing procedure includes material removal with 6 µm DLF. In this step, Si and $Ge_{1-x}Sn_x$ samples are thinned to equal thickness (~ 300 µm). Further polishing is continued with 3 µm and 1 µm DLF until the thickness is ~200 µm. With 1 µm DLF still attached to the rotary platen an angle of 1° (or 2°) is introduced. When the sample is ~80 µm thick the DLF is changed to 0.5 µm and the sample is further polished until the thickness of 10 µm. The dark red color of Si is becoming visible when the thickness is between 10 and 5 µm (see Figure 27. a)). As previously for Si samples, 0.1 µm DFL is used to polish both samples to electron transparency. The samples must be constantly checked under VLM so that the color changes of Silicon can be spotted, and the polishing procedure can be stopped when electron transparency is achieved.

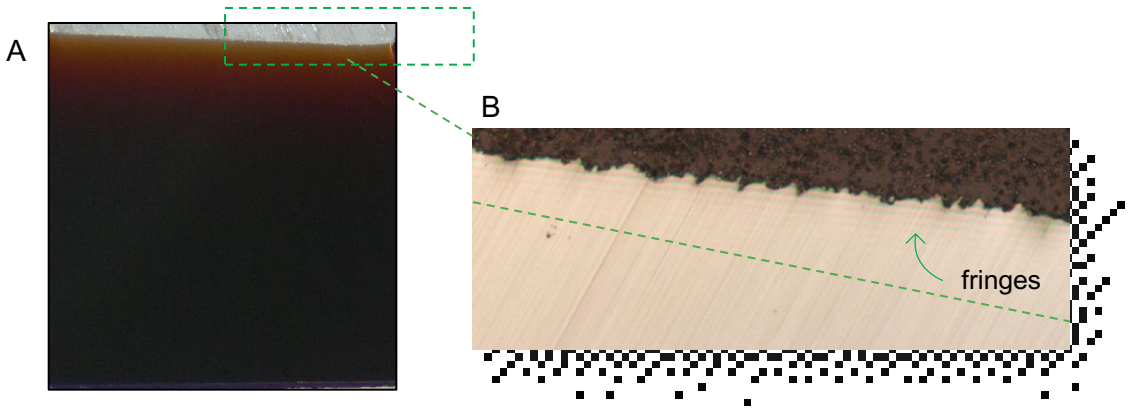

Figure 27. *VLM images of wedge polished Si sample. In a) the color changes from dark red to orange and yellow can be seen. b) Interference fringes appear in the thinnest area of the sample indicating electron transparency of the wedge sample.*

The Pyrex/TEM holder with glued prepared wedge polished sample is placed in a container with Acetone for a few hours to dissolve wax and to remove the sample from the glass. The wedge sample is cleaned with IPA, Microorganic soap, GP Cleaning Solution, and distilled water.

3.4. Scanning Electron Microscopy

It is necessary to investigate prepared samples with more detailed techniques than VLM to validate the developed sample preparation procedure. Here we use SEM to provide detailed images of the sample surface. The goal of any sample preparation procedure is to preserve the original surface of the material, its properties, and to prevent the introduction of artifacts. The SEM images provide information on the quality of the preparation procedure including the cleaning process of the sample and allow us to estimate the thickness of the final product. This information is a guideline to optimize the preparation method.

A copper ring has been cut out in two parts and the prepared wedge polished sample has been mounted to it gluing the thicker part of the sample to the copper “half ring”. The supporting half ring with the sample is inserted in SEM chamber to evaluate the quality of the prepared sample and consequently the wedge polishing procedure.

3.4.1. Cleaning routine optimization

Cleaning is another challenge in sample preparation. Firstly, only dipping into various solutions was used. Si and $Ge_{1-x}Sn_x$ samples were immersed for 15 minutes in Ac to dissolve the remaining wax. Cleaning was performed without any mechanical treatment of the sample. Microorganic Soap and distilled water were used afterward. The sample was immersed for 15 minutes at each cleaning step. Using SEM images, it has been realized that Acetone (if not properly removed) stays on the sample’s surface as stains (Figure 28). Hence, this information has been applied for the final cleaning of the sample and the cleaning protocol has been changed and adjusted.

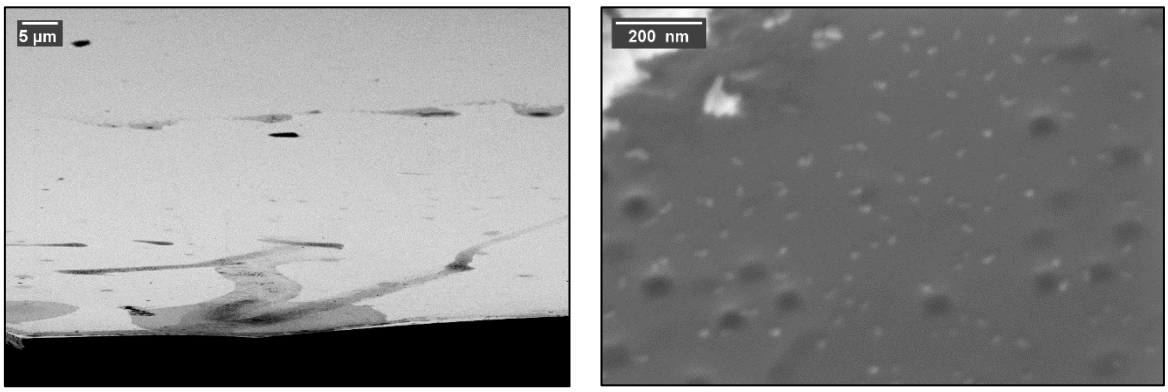

Figure 28. *SEM images of the prepared wedge samples with the residual of wax and cleaning solutions.*

The optimized cleaning routine still involved Ac to dissolve wax because it is quite efficient. But the residual acetone stains were removed by IPA. The wedge sample has been immersed into a container filled with IPA gently clean with few cotton fibres from a cotton swab. The cleaning was done under a stereomicroscope. IPA was exchanged several times to remove Ac stains and achieve a clean surface. Microorganic soap efficiently removes IPA and eliminates most organic impurities and it is exchanged several times as well. Another solution, GP Cleaning solution from Allied Tech was used for cleaning, because it was efficient in removing dust and residual of the previously used solutions. After this solution, a sample can be dried on paper or rinsed with distilled water and then dried. The cleaning procedure can be time-consuming. Nevertheless, it is better to invest time to properly clean the sample.

3.4.2. Quality of wedge polished sample

The quality of the polishing procedure can be estimated via SEM micrographs of the sample. Figure 29 presents SEM images of the prepared wedge sample. In the first SEM image in Figure 29 the sample is mounted on a half grid and viewed from a polished side. The edge of the sample is mostly uniform with occasional ruptures. The second SEM image (Figure 29 b)) represents a magnified thin edge. The measured thickness is ≈200 nm, but one can spot that the edge is not fully retained therefore thickness can vary.

A

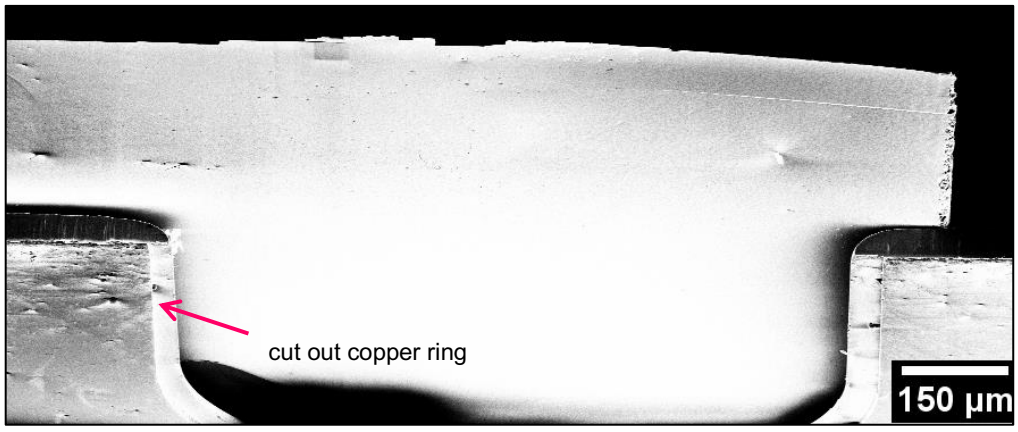

B

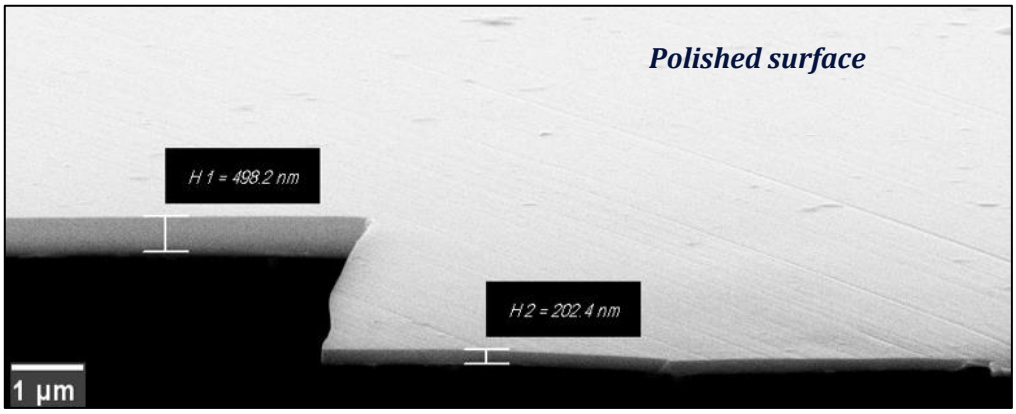

Figure 29. *SEM image of mounted wedge sample on a grid (A) and magnified image of the thinned edge prepared with wedge polishing procedure (B).*

From Figure 30. presenting SEM images of Si samples with Ge QDs it is visible that the surface is well preserved. Ge QDs are unaffected by the polishing procedure. The overall surface is clean and uniform with occasional dust particles and negligible dirt related to wax and cleaning solutions.

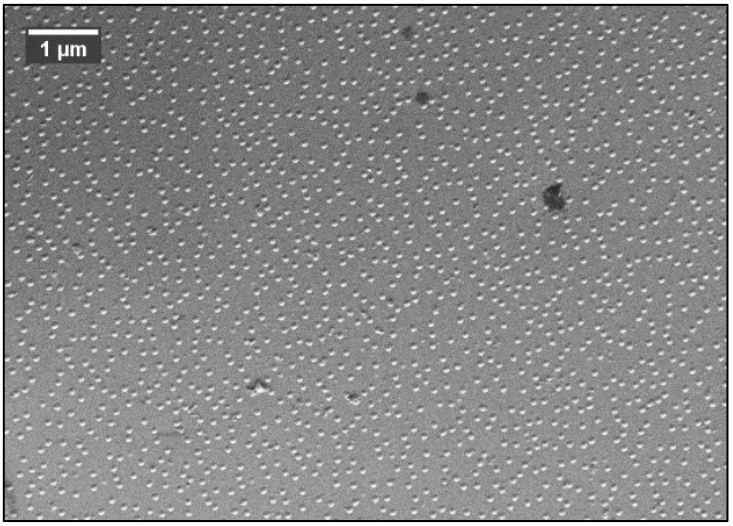

Figure 30. *Representative SEM images of the surface of Si wafer with Ge QD grown by molecular beam epitaxy after wedge polishing procedure.*

The Si and $Ge_{1-x}Sn_x$ samples were successfully prepared with the wedge polishing procedure. The surface of interest is preserved and mainly unaffected by the polishing procedure. The thin edge of the sample was mainly retained, although some deformation such as cracks and cleavage are present.

3.4.3. Preparation of MEMS-based Chip

The experiment aims to develop the procedure for the specimen preparation for *in situ* TEM experiment. The preparation of the heating chip should be a well-thought procedure to preserve material properties. Since a plan-view wedge polished sample is prepared it can be further used for the preparation of plan-view lamella.

Here a procedure on how to prepare a lamella in a dual FIB/SEM system and its subsequent transfer to the heating MEMS-based nano-chip using DENSsolution 54°/33° FIB stub (see Figure 31.) will be described.

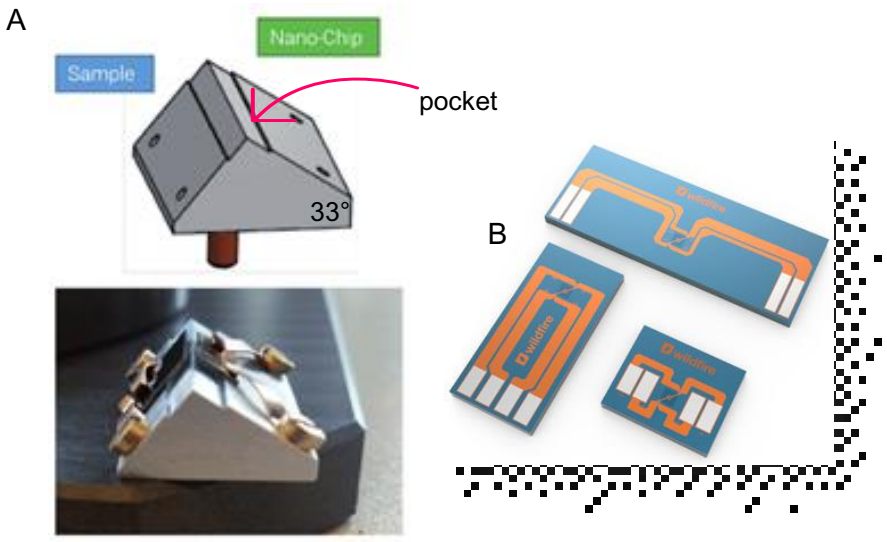

Figure 31. *a) Graphic of a FIB stub showing the "pocket" and an image of FIB stub; b) DENSsolution MEMS-based nano-chip.*

To preserve the epitaxial layer of $Ge_{1-x}Sn_x$ and shorten the preparation time of the chip the following procedure combines wedge polished sample preparation and the FIB technique. There are various methods and approaches to prepare a heating chip with a thin specimen. The plan-view lamella could be prepared from a thin wedge polished sample having edge thickness from a few hundreds of nanometres up to 1-2- micrometres. The wedge polished sample is mounted on a half grid and placed onto an SEM stub. SEM stub is mounted on an SEM holder. The nano-chip is usually positioned on the 33° side as Figure 31. Presents. But in this approach, the nano-chip is positioned outside the pocket of the FIB stub as can be seen in Figure 33. The chip preparation procedure can be divided into four steps: 1)

preliminary of plan-view lamella, 2) lift-out, 3) *in situ* transfer onto the MEMS chip, and 4) final thinning to electron transparency.

Two main points should be noted during the preparation of the lamella and transfer to the MEMS chip. Firstly, to preserve the surface of interest exposure to FIB and ion damage should be strictly avoided. Therefore, cutting the lamella and later thinning to electron transparency are both done from the backside of the sample where is the polished surface. Secondly, geometry inside the SEM/FIB chamber should be manipulated to facilitate the lift out and transfer of lamella and to preserve the surface of interest.

1) Preliminary thinning of plan-view lamella

The sample is viewed in SEM to find a proper surface to cut out lamella. After selecting the region of interest for the specimen preparation the micromanipulator and gas injector are inserted (see Figure 32. a). In this approach, a thicker wedge prepared sample is thinned to approximately 1 µm. A window is milled in the bulk sample with FIB to facilitate and to allow contact of the micromanipulator and predicted lamella.

The micromanipulator is brought into contact with the top left corner of the predicted lamella and welded to it with Pt (see Figure 32. b). Using FIB, a plane-view lamella is cut out from the region of interest. This procedure is known as lift out procedure.

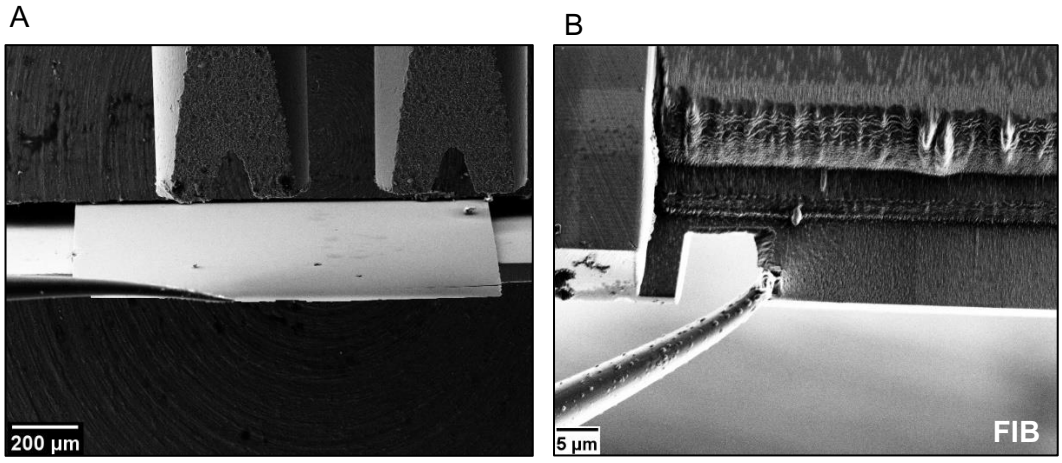

Figure 32. *a) Wedge sample mounted on a grid. GIS system and micromanipulator approaching the sample can be seen. b) Welded micromanipulator to the corner of the future lamella.*

2) Cutting of the lamella

The geometry inside the SEM/FIB chamber during the cutting procedure is shown in Figure 33. a). The angle between the FIB column and the SEM column is 54°. Keeping the surface of interest in the shadow from the ion beam the SEM stage is tilted and working distance is set at the eucentric point of SEM and FIB. In this position, we could see the same area of the sample in both SEM and FIB modes, additionally, the viewed sample area does not move drastically when the sample is tilted. Using FIB lamella is pre-cut out from the bulk sample, welded to the micromanipulator with ion-stimulated Pt deposition, and lift out.

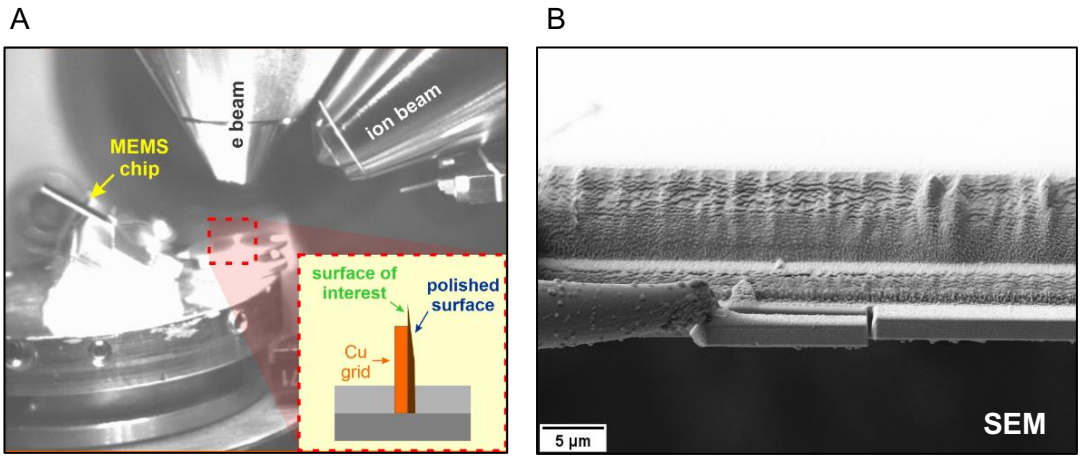

Figure 33. *a) In-chamber camera view inside the SEM/FIB during lift out. b) SEM images of the lift out procedure.*

3) Installation of the lamella to the MEMS chip

Manipulation of the SEM/FIB stage tilting should favour and facilitate the transfer procedure. The geometry inside the SEM/FIB chamber is presented in Figure 33. A), nevertheless depends on the system that is used. Rotating micromanipulator options as well facilitates the transfer. The lamella attached to the micromanipulator is transferred to the MEMS chip viewing window and welded from both sides with Pt (see Figure 33. b)). The lamella is intentionally welded on a slight angle (7°) to facilitate the last step of the procedure, the final thinning. The surface of interest is faced to the SiN membrane of the MEMS chip so that the thinning can be performed on the backside of the sample, therefore from the polished side. After securing lamella to the chip micromanipulator is detached.

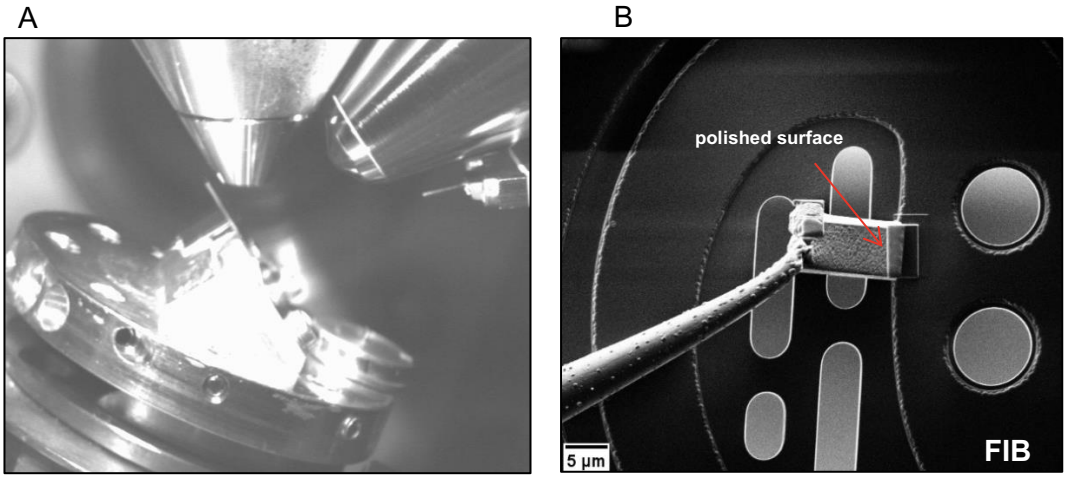

Figure 34. *In-chamber camera view during the transfer of the lamella onto the MEMS chip. B) FIB image of welded lamella to the SiN membrane of the nanochip.*

4) Final thinning of the specimen

The last step is to make lamella thin enough ready for the TEM investigation. The final thinning to ~200 nm is done by reducing the ion beam accelerating voltage and current from 30 kV 50 nA to 5 kV and 50 pA. Tilting is done respectively to the FIB column so that the stage is placed parallel to the FIB column and thinning can be performed (see geometry in Figure 35 a)). This geometry and position of the lamella on the MEMS chip facilitate final thinning and reduces the damage of the SiN membrane. The thinning with FIB is done gradually to preserve the surface of interest, maintain the material's properties, and to avoid ion damage caused by high voltage beam. Milling can be observed with SEM imaging and therefore if any unwanted events are occurring milling can be stopped.

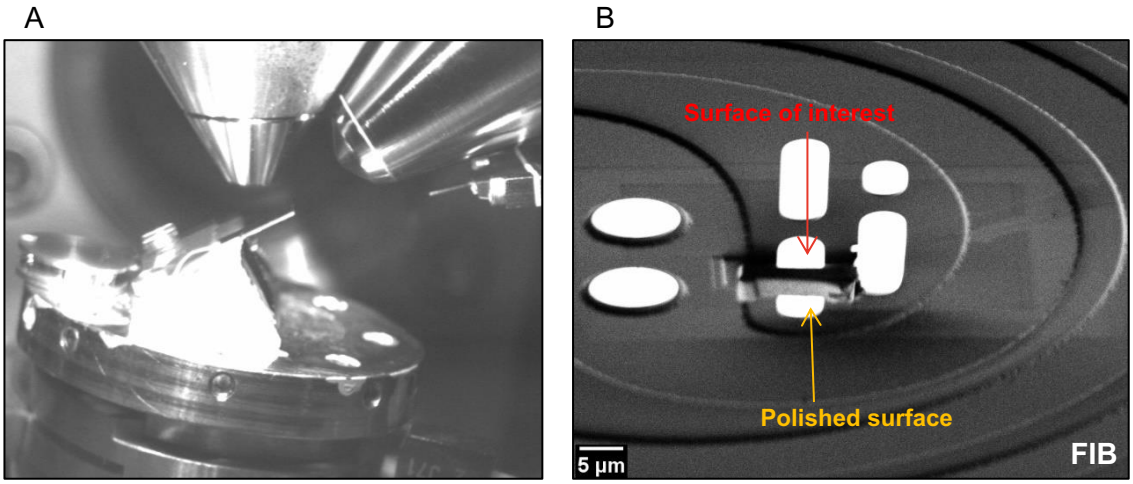

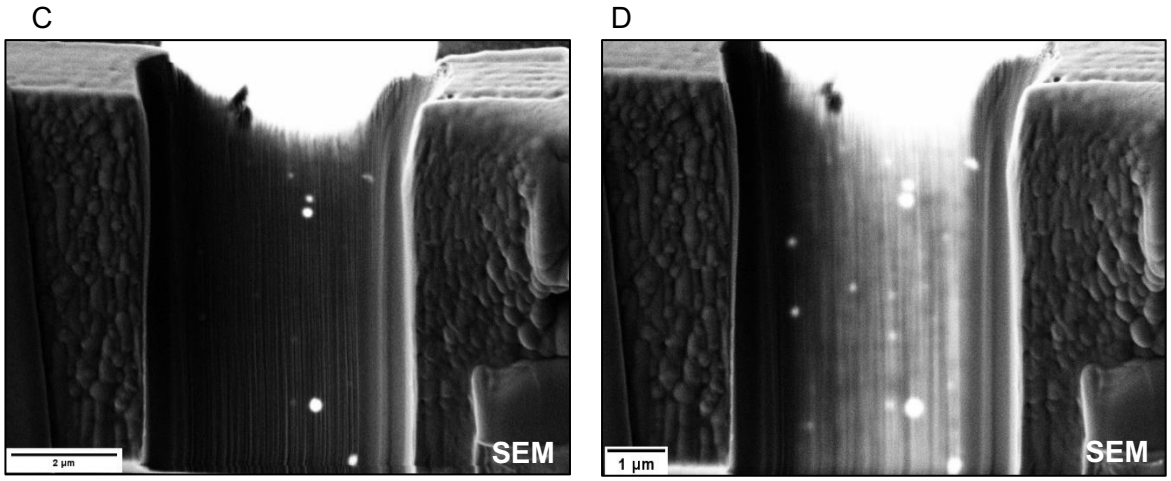

Figure 35 *a) In-chamber view inside SEM/FIB. b) FIB imaging mode of the orientation of the lamella welded to the chip. c) SEM image of the gradually thinned lamella. d) SEM image of the electron transparent area at 3kV.*

While thinning, the electron transparent area of the lamella appears brighter in the SEM image (see Figure 35. c) and d)). The appearance of more intensely transparent entities (white spots) during thinning of the lamellae corresponds to the deep holes present in the original epitaxial layer of $Ge_{1-x}Sn_x$ and it coincides with presented AFM images and topography 3D simulation of the same sample.

After a larger region is thinned to electron transparency the specimen is ready for the TEM experiment. Despite the procedure described here is specific to the used FIB system and MEMS-based heating holder it can be adapted to any other.

3.5. Validation of the sample preparation procedure

This section suits for merging the previously described work into a final experiment. Here the results of the first *in situ* experiment of Si sample will be presented.

Before proceeding with the *in situ* experiments the quality of the preparation procedure must be validated. The prepared MEMS-based chips with installed $Ge_{1-x}Sn_x$ specimen and Si specimen are checked in TEM at room temperature. The results of the preparation procedure are presented in Figure 36. The first image shows a Si sample with Ge QDs. As is it can be noted, the surface with QDs is preserved, it is clean, and Ge QDs are unaffected. The second image is obtained from a $Ge_{1-x}Sn_x$ sample with 10.5% Sn content and shows a preserved surface of interest. Both images show almost uniform thickness in the sample and there are no visible artifacts caused by the polishing procedure. We can confirm the cleanness and pristine nature of the transferred specimen.

The resulting TEM images correlate with the data obtained with AFM after the growth and with SEM images after the polishing procedure.

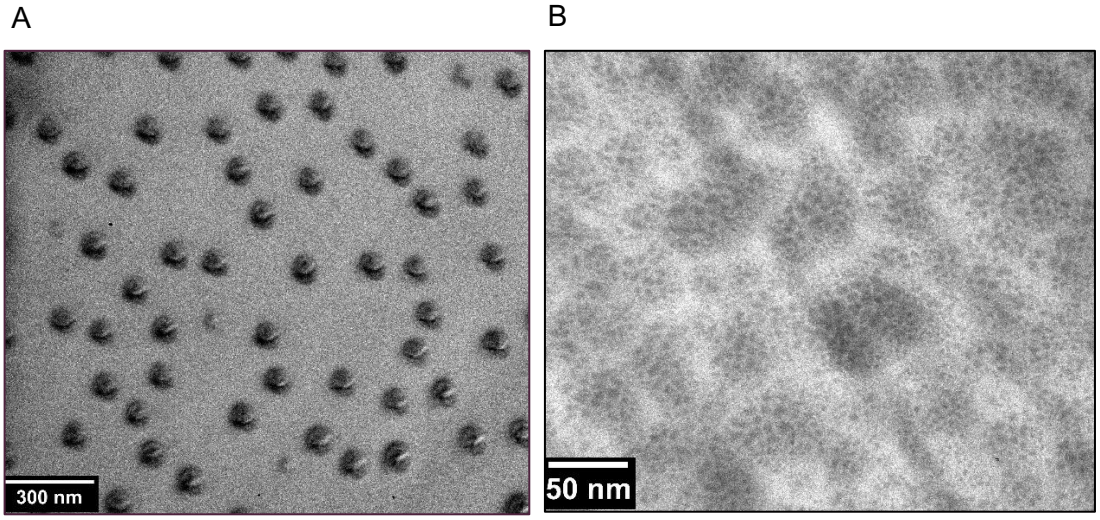

Figure 36. *TEM images (Zone axis alignment) of a) Si specimen with Ge QDs and b)* $Ge_{1-x}Sn_x$ *specimen installed on MEMS nanochip.*

3.5.1. *In situ* heating experiment

The first *in situ* heating TEM experiment was performed with Si test sample with Ge QDs. Observations of the behaviour of Si sample during *in situ* heating experiment are demonstrated and supported by a TEM image sequence (in Figure 37, from 1-8) of the same area of the sample at different temperatures varied in the 50-1000°C range. The heating environment is manipulated by *DENSSolutions* software.

To highlight the inherent strain of the QDs the investigation has been fulfilled in a specific specimen alignment, where one diffracted and the direct electron beam is present. For the investigation, a bright-field image of the direct beam was used. Microscopists commonly called it a two-beam condition. Nonetheless, the fundamentals of microscopic approaches justification and explanation of obtained scientific results are not in the frame of this master's thesis. Only several minor conclusions that should be presented are as follows.

At 50°C Ge QDs have a symmetrical "coffee-bean" shape. The dark "lines" present in the centre of the Ge islands are caused by the missing intensity of the diffracted beam in the direct beam. Also, due to the dual-beam imaging condition (direct and diffracted image), the introduction of additional strains and dislocations can be visualized by the change of this exact diffraction condition leading to a splitting of the above-mentioned "lines". As the chip and specimen are heated to a higher temperature more structural changes are visible within the Ge QD structures. Elevated temperature introduces more strains and dislocations to the structure which can be observed as curved structures within QD. After exceeding the threshold value for strains, QDs eventually undergo strain relaxation where defects are introduced to the structure. After heating, it is visible that defects are introduced, and thus the overall structure is changed. The melting point of Ge is 938.2°C and the images taken at 1000°C shows that the primary Ge QD structure is melted and changed.

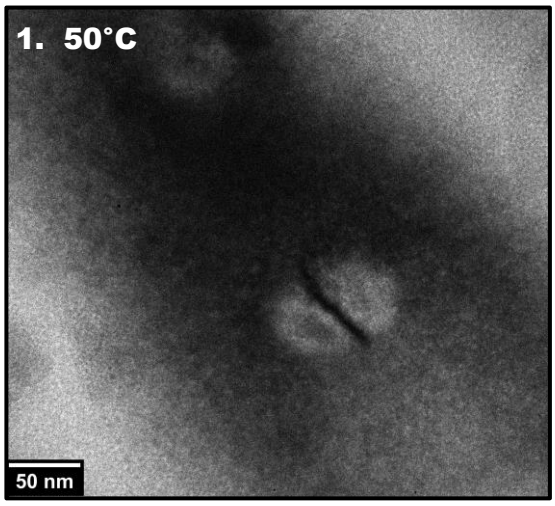
1. 50°C
50 nm

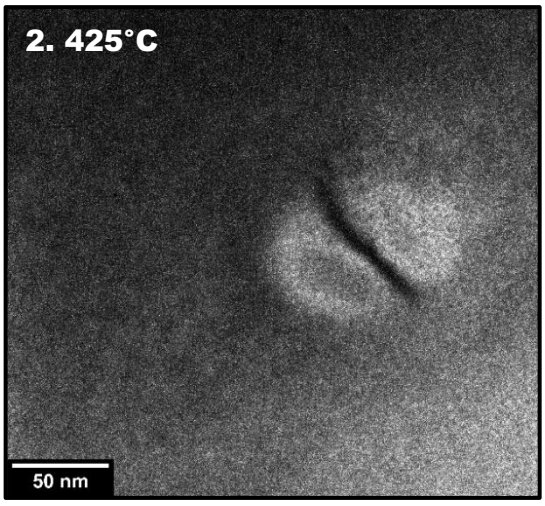
2. 425°C
50 nm

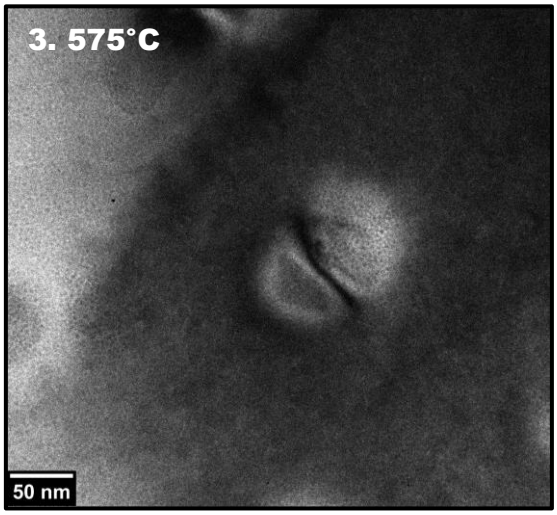
3. 575°C
50 nm

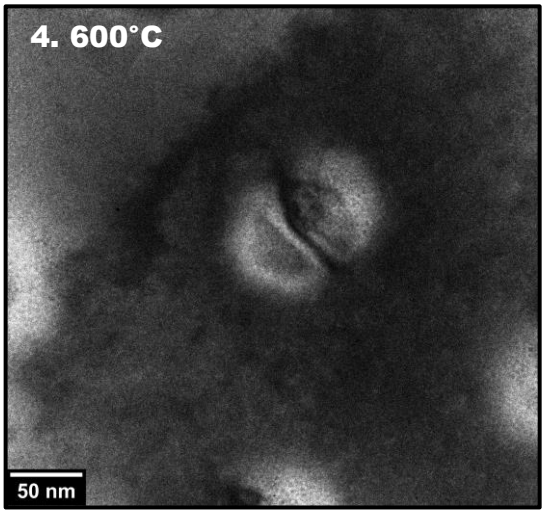
4. 600°C
50 nm

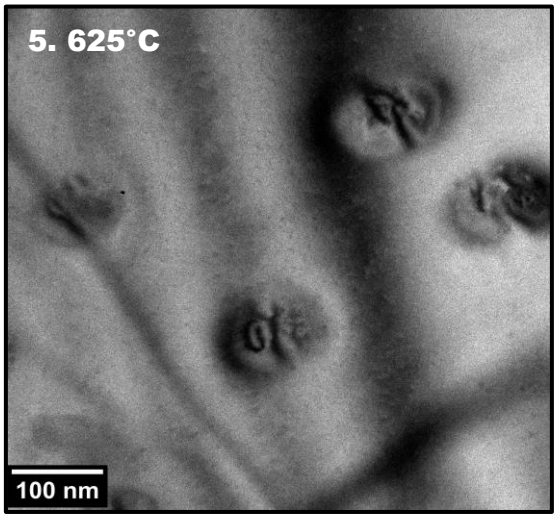
5. 625°C
100 nm

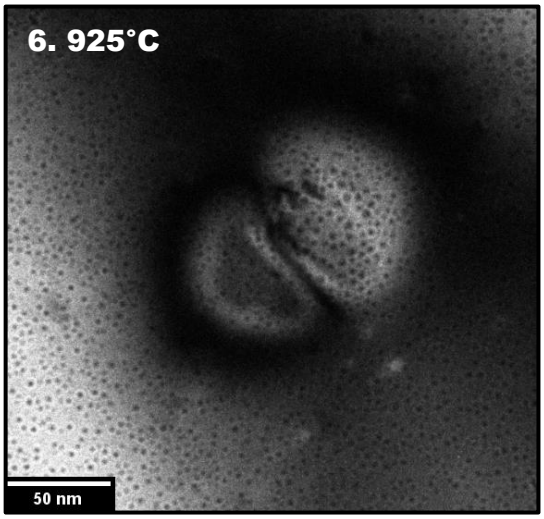
6. 925°C
50 nm

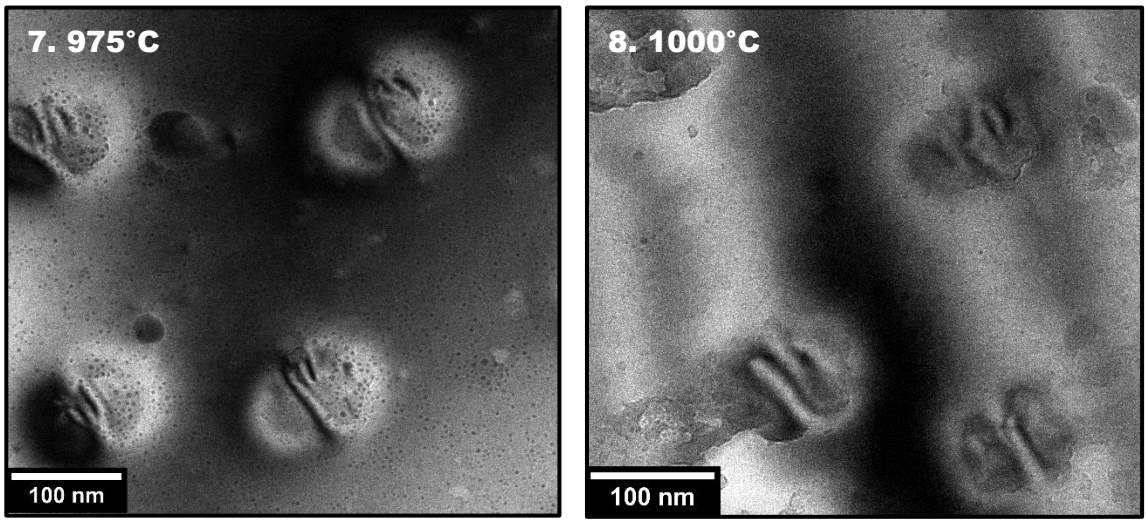

***Figure 37**. TEM images (two-beam alignment) of Si sample with Ge QD during in situ heating experiment with a temperature range from 50°C to 1000°C. The focus is on Ge QD and the evolution of strains within the structure*.

Based on the existing data and results on the first *in situ* heating experiment it can be concluded that the entire sample preparation procedure including wedge polishing preparation, FIB preparation of lamella, and installation to the MEMS chip were successful.

4. Conclusion

The goal of this master's thesis was to find a novel, practical way for sample preparation protocol to investigate the epitaxial $Ge_{1-x}Sn_x$ alloy and Si wafer with Ge QDs as reference material during an *in situ* heating TEM experiment. The sample preparation is a key step toward TEM investigation. Since the aim is to investigate the epitaxial layers which are nonequilibrium entities, the preparation method must be suitable to preserve the properties of the surface of interest. This thesis combines many aspects of sample preparation procedure to develop a novel approach for plan-view specimen preparation. The workflow for the sample preparation is in detail presented as well as the obstacles and challenges that were faced during the sample preparation. The starting point was to obtain a thin edge using the wedge polishing technique. Wedge polished samples were successfully achieved for both materials ($Ge_{1-x}Sn_x$ alloy and Si with Ge QDs). Special attention has been given to the thickness determination related problems and useful insides were given on possible solution to overcome this issue. The quality of prepared wedge sample was checked with VLM and SEM and further the wedge polished sample was used for the development of the preparation procedure for the *in situ* heating experiment. The wedge polishing improves the overall procedure as it reduces the time required to prepare the sample avoiding additional ion milling and it facilitates the preparation of plan-view lamella.

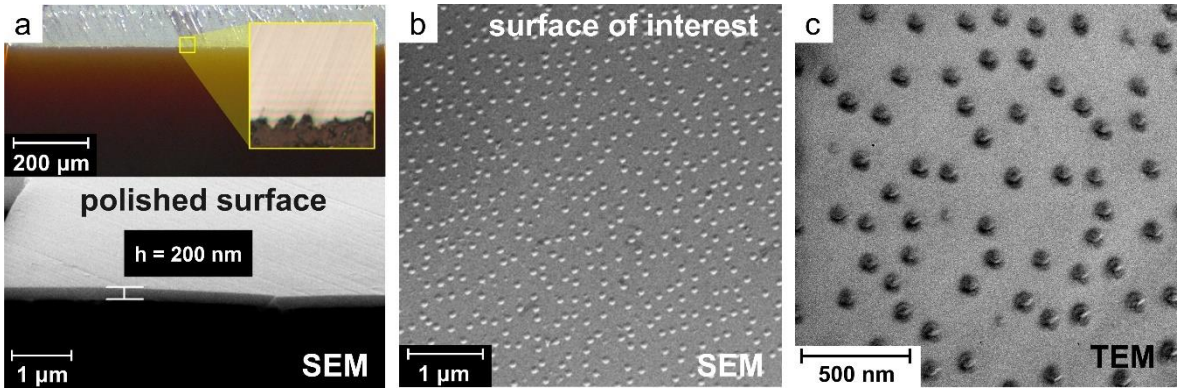

Figure 38. *Summarize characterization of the prepared Si sample with Ge QDs: a) VLM images of wedge polished sample and related SEM image of the achieved thin edge; b) SEM image of the surface of interest before proceeding with the preparation of lamella; c) Corresponding TEM image of the surface of interest after installation of the lamella to the chip.*

Figure 38 is presenting an outlook of the preliminary characterization of the prepared sample. Pre-characterization is presented through VLM, SEM, and TEM images to provide

analytical validation of the sample preparation procedure. More peculiarly the key point is to present retention of the original surface of interest and to show the intact structural surface components through the whole process. In this case, Ge QDs are unaffected by the wedge polishing procedure which can be seen in SEM images (see Figure 38. b), and we managed to retain the QDs structure after the preparation of lamella and its installation to the MEMS heating chip, which has been confirmed by TEM examination at room temperature (see Figure 38. c) and Figure 39. d)).

Two approaches are possible to prepare a plan-view lamella starting from the wedge sample. One involves an already thin edge and immediate cutting with FIB and the other involves preparing a slightly thicker wedge sample and additional thinning with the ion beam. The installation of lamella on cutting-edge MEMS-based chip was thrivingly prepared, as it has been presented. The chip preparation procedure is described for the available SEM/FIB system and equipment, but it can be adapted to any other. Figure 39 outlines the crucial steps in the chip preparation procedure, showing the cutting of the lamella (a), its subsequent installation on the MEMS chip (b), and the final thinning (c) to electron transparency. The most important outcome that must be emphasized is that the surface of interest was not altered by the wedge polishing procedure nor the FIB preparation. Therefore, the TEM image of a thin specimen presented in Figure 39 c) has been obtained to confirm that the surface of interest corresponds to the previously obtained SEM images. The quality of the prepared chip and therefore of the overall procedure is satisfactory.

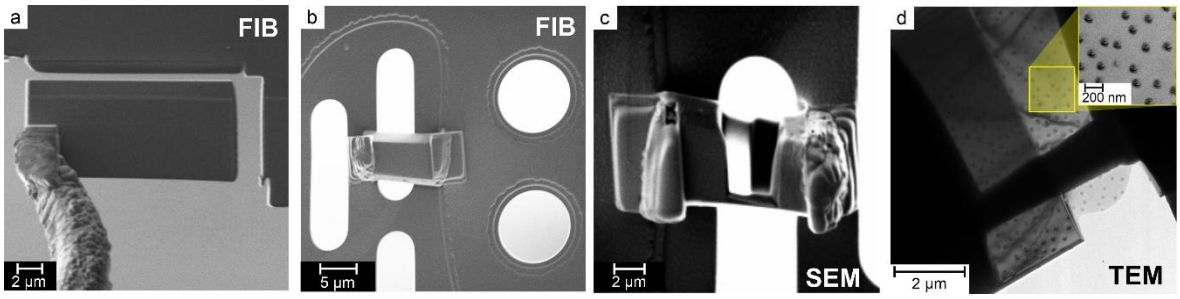

Figure 39. *An outlook of the preparation of the MEMS heating chip, a) lift out; b) installation of the lamella on the MEMS heating chip; c) final thinning to electron transparency; and d) validation of the prepared chip with Si sample with Ge QDs with TEM.*

The results of the first *in situ* heating experiment are presented and evaluated. The results obtained in this master's thesis research project could serve as a guideline for further development and optimization of the sample preparation procedure for *in situ* heating experiments.

5. References

[1] J. Doherty *et al.*, “Influence of growth kinetics on Sn incorporation in direct band gap $Ge_{1-x}Sn_x$ nanowires,” *J. Mater. Chem. C*, vol. 6, no. 32, pp. 8738–8750, 2018, DOI: 10.1039/c8tc02423e.

[2] S. Wirths *et al.*, “Lasing in direct-bandgap GeSn alloy grown on Si,” *Nat. Photonics*, vol. 9, no. 2, pp. 88–92, 2015, DOI: 10.1038/nphoton.2014.321.

[3] H. Groiss *et al.*, “Free-running Sn precipitates: An efficient phase separation mechanism for metastable $Ge_{1-x}Sn_x$ epilayers,” *Sci. Rep.*, vol. 7, no. 1, pp. 1–12, 2017, DOI: 10.1038/s41598-017-16356-8.

[4] R. J. Alan Esteves, S. Hafiz, D. O. Demchenko, Ü. Özgür, and I. U. Arachchige, “Ultra-small $Ge_{1-x}Sn_x$ quantum dots with visible photoluminescence,” *Chem. Commun.*, vol. 52, no. 78, pp. 11665–11668, 2016, DOI: 10.1039/c6cc04242b.

[5] S. Assali *et al.*, “Kinetic Control of Morphology and Composition in Ge/GeSn Core/Shell Nanowires,” *ACS Nano*, vol. 14, no. 2, pp. 2445–2455, 2020, DOI: 10.1021/acsnano.9b09929.

[6] R. J. A. Esteves, M. Q. Ho, and I. U. Arachchige, “Nanocrystalline group IV alloy semiconductors: Synthesis and characterization of Ge1- xSnx quantum dots for tunable bandgaps,” *Chem. Mater.*, vol. 27, no. 5, pp. 1559–1568, 2015, DOI: 10.1021/cm503983b.

[7] D. B. Williams and C. B. Carter, *Transmission electron microscopy: A textbook for materials science*. 2009.

[8] R. T. G and A. B. R, “Transmission Electron Microscopy - An Overview,” *Int. Res. J. Invent. Trasnmission Electron Microsc.*, no. March, 2019.

[9] J. Ayache, L. Beaunier, J. Boumendil, G. Ehret, and D. Laub, *Sample Preparation Handbook for Transmission Electron Microscopy - Technology*. 2010.

[10] J. Ayache, L. Beaunier, J. Boumendil, G. Ehret, and D. Laub, *Sample Preparation Handbook for Transmission Electron Microscopy*. Springer New York, 2010.

[11] Y. Rong, *Characterization of Microstructures by Analytical Electron Microscopy (AEM)*. Springer Berlin Heidelberg, 2012.

[12] A. Romano, J. Vanhellemont, and H. Bender, “A Fast and Precise Specimen Preparation Technique for TEM Investigation of Prespecified Areas of Semiconductor Devices,” *MRS Proc.*, vol. 199, no. 4, pp. 223–224, 1990, DOI: 10.1557/proc-199-167.

[13] L. Pavesi, L. Dal Negro, C. Mazzoleni, G. Franzò, and F. Priolo, “Optical gain in silicon nanocrystals,” *Nature*, 2000, DOI: 10.1038/35044012.

[14] J. R. Sánchez-Pérez *et al.*, “Direct-bandgap light-emitting germanium in tensilely

strained nanomembranes," *Proc. Natl. Acad. Sci. U. S. A.*, 2011, DOI: 10.1073/pnas.1107968108.

[15] R. W. Olesinski and G. J. Abbaschian, "The $Ge_{1-x}Sn_x$ (Germanium-Tin) system," *Bull. Alloy Phase Diagrams*, 1984, DOI: 10.1007/BF02868550.

[16] A. Barron, "Structures of Element and Compound Semiconductors," *OpenStax-CNX*, 2009. http://cnx.org/content/m23905/1.6/ (accessed Jul. 21, 2020).

[17] A. Nylandsted Larsen, "Epitaxial growth of Ge and SiGe on Si substrates," *Mater. Sci. Semicond. Process.*, 2006, DOI: 10.1016/j.mssp.2006.08.039.

[18] U. Mark Winter (The University of She eld and WebElements Ltd, "WebElements - The Periodic Table." https://www.webelements.com/.

[19] S. Gupta, B. Magyari-Köpe, Y. Nishi, and K. C. Saraswat, "Achieving direct band gap in germanium through integration of Sn alloying and external strain," *J. Appl. Phys.*, 2013, DOI: 10.1063/1.4792649.

[20] Y. Kawamura *et al.*, "Direct-gap photoluminescence from germanium nanowires," *Phys. Rev. B - Condens. Matter Mater. Phys.*, 2012, DOI: 10.1103/PhysRevB.86.035306.

[21] W. Sun *et al.*, "Size-Tunable Photothermal Germanium Nanocrystals," *Angew. Chemie - Int. Ed.*, 2017, DOI: 10.1002/anie.201701321.

[22] P. Moontragoon, Z. Ikonić, and P. Harrison, "Band structure calculations of Si- $Ge_{1-x}Sn_x$ alloys: Achieving direct band gap materials," *Semicond. Sci. Technol.*, 2007, DOI: 10.1088/0268-1242/22/7/012.

[23] S. Assali *et al.*, "Growth and Optical Properties of Direct Band Gap Ge/Ge0.87Sn0.13 Core/Shell Nanowire Arrays," *Nano Lett.*, vol. 17, no. 3, pp. 1538–1544, 2017, DOI: 10.1021/acs.nanolett.6b04627.

[24] T. T. Tran, J. Mathews, and J. S. Williams, "Towards a direct band gap group IV Ge-based material," *Materials Science in Semiconductor Processing*. 2019, DOI: 10.1016/j.mssp.2018.05.037.

[25] J. Zheng *et al.*, "Growth of high-Sn content (28%) GeSn alloy films by sputtering epitaxy," *J. Cryst. Growth*, 2018, DOI: 10.1016/j.jcrysgro.2018.04.008.

[26] S. H. Na and C. H. Park, "First-principles study of the structural phase transition in Sn," *J. Korean Phys. Soc.*, vol. 56, no. 12, pp. 494–497, 2010, DOI: 10.3938/jkps.56.494.

[27] A. A. Tonkikh, N. D. Zakharov, A. A. Suvorova, C. Eisenschmidt, J. Schilling, and P. Werner, "Cubic phase Sn-rich GeSn nanocrystals in a Ge matrix," *Cryst. Growth Des.*, 2014, DOI: 10.1021/cg401652f.

[28] S. Zaima, O. Nakatsuka, N. Taoka, M. Kurosawa, W. Takeuchi, and M. Sakashita, "Growth and applications of GeSn-related group-IV semiconductor materials,"

Science and Technology of Advanced Materials. 2015, DOI: 10.1088/1468-6996/16/4/043502.

[29] S. Wirths, D. Buca, and S. Mantl, "Si- $Ge_{1-x}Sn_x$ alloys: From growth to applications," *Progress in Crystal Growth and Characterization of Materials*. 2016, DOI: 10.1016/j.pcrysgrow.2015.11.001.

[30] M. Oehme, K. Kostecki, M. Schmid, F. Oliveira, E. Kasper, and J. Schulze, "Epitaxial growth of strained and unstrained GeSn alloys up to 25% Sn," *Thin Solid Films*, 2014, DOI: 10.1016/j.tsf.2013.10.064.

[31] J. Kouvetakis, J. Menendez, and A. V. G. Chizmeshya, "Tin-based group IV semiconductors: New platforms for opto- and microelectronics on silicon," *Annu. Rev. Mater. Res.*, 2006, DOI: 10.1146/annurev.matsci.36.090804.095159.

[32] S. Gupta, "Germanium-Tin (Gesn) Technology," *Dissertation*, vol. دانشکده مه, no. August, p. 173, 2013.

[33] P. R. Pukite, A. Harwit, and S. S. Iyer, "Molecular beam epitaxy of metastable, diamond structure Sn xGe1-x alloys," *Appl. Phys. Lett.*, 1989, DOI: 10.1063/1.101152.

[34] H. Li, C. Chang, T. P. Chen, H. H. Cheng, Z. W. Shi, and H. Chen, "Characteristics of Sn segregation in Ge/GeSn heterostructures," *Appl. Phys. Lett.*, 2014, DOI: 10.1063/1.4898583.

[35] H. Li, Y. X. Cui, K. Y. Wu, W. K. Tseng, H. H. Cheng, and H. Chen, "Strain relaxation and Sn segregation in GeSn epilayers under thermal treatment," *Appl. Phys. Lett.*, 2013, DOI: 10.1063/1.4812490.

[36] S. Biswas *et al.*, "Non-equilibrium induction of tin in germanium: Towards direct bandgap Ge 1-x Snx nanowires," *Nat. Commun.*, 2016, DOI: 10.1038/ncomms11405.

[37] C. Z. N. Peidong Yang, L. Dou, and P. Yang, "Bandgap engineering in semiconductor alloy nanomaterials with widely tunable compositions," *Nature Reviews Materials*. 2017, DOI: 10.1038/natrevmats.2017.70.

[38] J. Doherty *et al.*, "Progress on Germanium-Tin Nanoscale Alloys," *Chem. Mater.*, 2020, DOI: 10.1021/acs.chemmater.9b04136.

[39] O. Gurdal *et al.*, "Low-temperature growth and critical epitaxial thicknesses of fully strained metastable $Ge_{1-x}Sn_x$ ($x \lesssim 0.26$) alloys on Ge(001)2×1," *J. Appl. Phys.*, 1998, DOI: 10.1063/1.366690.

[40] A. Y. Cho and J. R. Arthur, "Molecular beam epitaxy," *Prog. Solid State Chem.*, 1975, DOI: 10.1016/0079-6786(75)90005-9.

[41] J. Y. Tsao, *Materials Fundamentals of Molecular Beam Epitaxy*. 2012.

[42] J. R. Arthur, "Molecular beam epitaxy," *Surf. Sci.*, 2002, DOI: 10.1016/S0039-

6028(01)01525-4.

[43] P. J. Goodhew and J. Humphreys, “Electron Microscopy and Analysis, Third Edition,” *Electron Microsc. Anal.*, p. 264, 2014, DOI: 10.1201/9781482289343.

[44] “Francis Leonard Deepak, Alvaro Mayoral, Raul Arenal-Advanced Transmission Electron Microscopy_ Applications to Nanomaterials-Springer (2015).”

[45] N. Erdman, D. C. Bell, and R. Reichelt, “Scanning electron microscopy,” in *Springer Handbooks*, 2019.

[46] R. Kralj Janecek M., *Modern Electron Microscopy*. 2016.

[47] B. J. Inkson, “Scanning Electron Microscopy (SEM) and Transmission Electron Microscopy (TEM) for Materials Characterization,” in *Materials Characterization Using Nondestructive Evaluation (NDE) Methods*, 2016.

[48] W. Zhou, R. Apkarian, Z. L. Wang, and D. Joy, “Fundamentals of scanning electron microscopy (SEM),” in *Scanning Microscopy for Nanotechnology: Techniques and Applications*, 2007.

[49] P. Echlin, *Handbook of Sample Preparation for Scanning Electron Microscopy and X-Ray Microanalysis*. 2009.

[50] W. Sigle, “Analytical transmission electron microscopy,” *Annual Review of Materials Research*. 2005, DOI: 10.1146/annurev.matsci.35.102303.091623.

[51] F. Krumeick, “Properties of electrons, their interactions with matter and applications in electron microscopy,”, 2011.

[52] J. Kacher, B. P. Eftink, and I. M. Robertson, “In situ transmission electron microscopy investigation of dislocation interactions,” in *Handbook of Mechanics of Materials*, 2019.

[53] F. M. Ross and A. M. Minor, “In situ transmission electron microscopy,” in *Springer Handbooks*, 2019.

[54] P. J. Ferreira, K. Mitsuishi, and E. A. Stach, “In Situ Transmission Electron Microscopy,” *MRS Bull.*, 2008, DOI: 10.1557/mrs2008.20.

[55] M. Zhang *et al.*, “In situ transmission electron microscopy studies enabled by microelectromechanical system technology,” *J. Mater. Res.*, 2005, DOI: 10.1557/JMR.2005.0225.

[56] “JEM-2200FS Field Emission Electron Microscope.” https://www.jeol.co.jp/en/products/detail/JEM-2200FS.html (accessed Sep. 21, 2020).

[57] D. Ayache, J., Beaunier, L., Boumendil, J., Ehret, G., Laub, *Sample Preparation Handbook*. 2010.

[58] D. V. S. Rao, K. Muraleedharan, and C. J. Humphreys, “TEM specimen preparation

techniques," *Microsc. Sci. Technol. Appl. Educ.*, 2010, DOI: 10.1007/BF02645554.

[59] F. L. Deepak, A. Mayoral, and R. Arenal, *Francis Leonard Deepak, Alvaro Mayoral, Raul Arenal-Advanced Transmission Electron Microscopy - Applications to Nanomaterials-Springer (2015)*. 2015.

[60] R. Komanduri, D. A. Lucca, and Y. Tani, "Technological advances in fine abrasive processes," *CIRP Ann. - Manuf. Technol.*, 1997, DOI: 10.1016/S0007-8506(07)60880-4.

[61] S. K. Curtis and P. J. Goodhew, "Specimen Preparation for Transmission Electron Microscopy of Materials," *Trans. Am. Microsc. Soc.*, 1985, DOI: 10.2307/3226447.

[62] W. C. Elmore, "Electrolytic polishing," *J. Appl. Phys.*, 1939, DOI: 10.1063/1.1707257.

[63] J. Ayache *et al.*, "Artifacts in Transmission Electron Microscopy," in *Sample Preparation Handbook for Transmission Electron Microscopy*, 2010.

[64] "Precision Polishing - Diamond Lapping Films." https://precision-polishing.com/en/news/diamond-lapping-film (accessed Oct. 10, 2020).

[65] L. A. Giannuzzi and F. A. Stevie, "A review of focused ion beam milling techniques for TEM specimen preparation," *Micron*, 1999, DOI: 10.1016/S0968-4328(99)00005-0.

[66] P. R. Munroe, "The application of focused ion beam microscopy in the material sciences," *Materials Characterization*. 2009, DOI: 10.1016/j.matchar.2008.11.014.

[67] J. I. Goldstein, D. E. Newbury, J. R. Michael, N. W. M. Ritchie, J. H. J. Scott, and D. C. Joy, *Microscopy and X-Ray Microanalysis*. 2007.

[68] J. Mayer, L. A. Giannuzzi, T. Kamino, and J. Michael, "TEM sample preparation and FIB-induced damage," *MRS Bull.*, 2007, DOI: 10.1557/mrs2007.63.

[69] M. Sezen, "Focused Ion Beams (FIB) — Novel Methodologies and Recent Applications for Multidisciplinary Sciences," in *Modern Electron Microscopy in Physical and Life Sciences*, 2016.

[70] N. I. Kato, "Reducing focused ion beam damage to transmission electron microscopy samples," *Journal of Electron Microscopy*. 2004, DOI: 10.1093/jmicro/dfh080.

[71] J. P. McCaffrey, M. W. Phaneuf, and L. D. Madsen, "Surface damage formation during ion-beam thinning of samples for transmission electron microscopy," *Ultramicroscopy*, 2001, DOI: 10.1016/S0304-3991(00)00096-6.

[72] S. Vijayan, J. R. Jinschek, S. Kujawa, J. Greiser, and M. Aindow, "Focused Ion Beam Preparation of Specimens for Micro-Electro-Mechanical System-based Transmission Electron Microscopy Heating Experiments," *Microsc. Microanal.*, 2017, DOI: 10.1017/S1431927617000605.

[73] J. W. Judy, "Microelectromechanical systems (MEMS): Fabrication, design and applications," *Smart Mater. Struct.*, 2001, DOI: 10.1088/0964-1726/10/6/301.

[74] M. A. Haque, H. D. Espinosa, and H. J. Lee, “MEMS for in situ testing - Handling, actuation, loading, and displacement measurements,” *MRS Bull.*, 2010, DOI: 10.1557/mrs2010.570.

[75] DENSSolutions, “Wildfire heating holder.” https://f.hubspotusercontent30.net/hubfs/469089/Brochures/DENSsolutions Wildfire Brochure Aug. 2020.pdf?utm_medium=email&_hsenc=p2ANqtz-9oj-BNSxaBSVIEihrmGMyrg8hVHf_EVxamBNcwSjumoxzXBupVUhMxg5A9ChVNvoYuUiKaTCbEZlmMjY7gYnBAimUxhA&_hsmi=72116780&utm_content (accessed Oct. 20, 2020).

[76] E. Meyer, “Atomic force microscopy,” *Prog. Surf. Sci.*, 1992. DOI: 10.1016/0079-6816(92)90009-7.

[77] G. Meyer and N. M. Amer, “Novel optical approach to atomic force microscopy,” *Appl. Phys. Lett.*, 1988, DOI: 10.1063/1.100061.

6. Curriculum Vitae

Natalija Šantić

linkedin.com/in/natalija-šantić

01 EDUCATION

MASTER'S DEGREE IN CHEMISTRY
@Department of Chemistry, Josip Juraj Strossmayer, Osijek
Croatia, *Sep 2018 - Nov 2020*
Thesis: "*In situ transmission electron microscopy (TEM) investigation of the decomposition of the epitaxial* $Ge_{1-x}Sn_x$ *layer*".

BACHELOR'S DEGREE IN CHEMISTRY
@Department of Chemistry, Josip Juraj Strossmayer, Osijek
Croatia, *Sep 2013 - Sep 2018*
Thesis: "*Synthesis of Neutral Complexes of Copper and Vanadium with Hydroxypyrones*".

02 EMPLOYMENT HISTORY

MASTER'S THESIS PROJECT
@CDL for Nanoscale Phase Transformations - JKU Linz
Feb 2020- Oct 2020

INTERNSHIP TRAINEE
@Center of Surface and Nanoanalytics - JKU Linz
July 2019 - Oct 2019

- Material investigation with a spotlight on Surface Science via modern analytical tools (TEM, SEM, AFM, KFM)
- Characterization of steel sample, semiconductors (Si, Ge, GeSn), and polymers (polyethylene, polytetrafluoroethylene).
- Technical experience in the sample preparation techniques in Material Science
- Plasma treatment of polymers and investigation of the surface modification.

03 EXTRA-CURRICULAR ACTIVITIES

STUDENT CAMP
@ WOOD K PLUS AND GRAZ UNIVERSITY OF TECHNOLOGY
Feb 2019
International Student camp on the topic of biorefineries and bio-based industrial products. The student camp focused on plant biomass used as raw material to produce a range of products spanning from fuels and fertilizers to chemicals, polymers, adhesives, and energy.

Volunteering
@IAESTE Croatia
Oct 2018 – Present
IAESTE is a non-profit organization offering a technical experience for STEM students worldwide and I have been devoted to volunteering for over 2 years.

- The volunteering helped me to elevate my skills in Leadership, Coordination of teams, and professional communication as I worked in various teams.
- Learnt to improvise and to quickly allocate.

International Conference
17th Ružička days "Today Science - Tomorrow Industry"
Oct 2018
Poster section on topic "Adsorption of hydrophilically modified silicones on oxide nanoparticles".

Symposium of Chemistry Students
@Faculty of Science
Sep 2018
Poster section on Bachelor thesis topic "Synthesis of Neutral Complex of Copper and Vanadium with Hydroxypyrones".

04 LANGUAGES

Language	Proficiency
Croatian	Mother language
English	B2
Italian	B1
German	A1